BBA - Biomembranes 1862 (2020) 183236

Contents lists available at ScienceDirect

BBA - Biomembranes

journal homepage: www.elsevier.com/locate/bbamem

Enhancing the membrane activity of Piscidin 1 through peptide metallation and the presence of oxidized lipid species: Implications for the unification of host defense mechanisms at lipid membranes

Steven D. Paredes[a], Sarah Kim[b], Mary T. Rooney[a], Alexander I. Greenwood[a], Kalina Hristova[b], Myriam L. Cotten[a,*]

[a] Department of Applied Science, William & Mary, Williamsburg, VA, United States
[b] Department of Materials Science and Engineering and Program in Molecular Biophysics, Hopkins University, Baltimore, MD, United States

ARTICLE INFO

Keywords:
Host defense peptides
Antimicrobial peptides
Copper-binding peptides
Membrane activity
Lipid partitioning
Solid-state NMR

ABSTRACT

Piscidins are host-defense peptides (HDPs) from fish that exhibit antimicrobial, antiviral, anti-cancer, anti-inflammatory, and wound-healing properties. They are distinctively rich in histidine and contain an amino terminal copper and nickel (ATCUN) binding motif due to the presence of a conserved histidine at position 3. Metallation lowers their total charge and provides a redox center for the formation of radicals that can convert unsaturated fatty acids (UFAs) into membrane-destabilizing oxidized phospholipids (OxPLs). Here, we focus on P1, a particularly membrane-active isoform, and investigate how metallating it and making OxPL available influence its membrane activity. First, we quantify through dye leakage experiments the permeabilization of the apo- and holo-forms of P1 on model membranes containing a fixed ratio of anionic phosphatidylglycerol (PG) and zwitterionic phosphatidylcholine (PC) but varying amounts of Aldo-PC, an OxPL derived from the degradation of several UFAs. Remarkably, metallating P1 increases membranolysis by a factor of five in each lipid system. Conversely, making Aldo-PC available improves permeabilization by a factor of two for each peptide form. Second, we demonstrate through CD-monitored titrations that the strength of the peptide-membrane interactions is similar in PC/PG and PC/PG/Aldo-PC. Thus, peptide-induced membrane activity is boosted by properties intrinsic to the peptide (e.g., charge and structural changes associated with metallation) and bilayer (e.g., reversal of sn-2 chain due to oxidation). Third, we show using oriented-sample ^{15}N solid-state NMR that the helical portion of P1 lies parallel to the bilayer surface in both lipid systems. ^{31}P NMR experiments show that both the apo- and holo-states interact more readily with PC in PC/PG. However, the presence of Aldo-PC renders the holo-, but not the apo-state, more specific to PG. Hence, the membrane disruptive effects of P1 and its specificity for the anionic lipids found on pathogenic cell membrane surfaces are simultaneously optimized when it is metallated and the OxPL is present. Overall, this study deepens our insights into how OxPLs affect peptide-lipid interactions and how host defense metallopeptides could help integrate the effects of antimicrobial agents.

1. Introduction

Biological membranes and their constituents are implicated in virtually all processes vital to living organisms [1–3]. The dependence of cell membrane functionality on the intertwined properties of its lipids, proteins, and surrounding environment is both captivating and challenging to investigate given the chemical diversity of the components and the technical challenges associated with their characterization

Abbreviations: AAA, amino acid analysis; Aldo-PC, 1-palmitoyl-2-(9'-oxo-nonanoyl)-sn-glycero-3-phosphocholine; ANTS, 8-aminonaphthalene-1,2,3-trisulfonic acid; ATCUN, amino terminal nickel and copper binding motif; CP, cross polarization; CSA, chemical shift anisotropy; DPX, *p*-xylylenebis(pyridinium bromide; EC_{50}, effective concentration of peptide yielding 50% leakage; *E*-field, electrical field; HDP, host defense peptide; LUVs, large unilamellar vesicles; MIC, minimum inhibitory concentration; OCD, oriented CD; OxPL, oxidized lipid; P1, piscidin 1; P3, piscidin 3; PC, phosphatidylcholine; PE, phosphatidylethanolamine; PG, phosphatidylglycerol; P/L, peptide-to-lipid ratio; POPC, 1-palmitoyl-2-oleoyl-glycero-3-phosphocholine; POPG, 1-palmitoyl-2-oleoyl-sn-glycero-3-phosphoglycerol; PUFA, polyunsaturated fatty acids; Q, peptide charge; ROS, reactive oxygen species; S-state, surface-bound state; SUVs, small unilamellar vesicles; T-state, tilted-state; UFA, unsaturated fatty acid

* Corresponding author at: 540 Landrum Drive, William & Mary, Department of Applied Science, Williamsburg, VA 23185, United States.
E-mail address: mcotten@wm.edu (M.L. Cotten).

https://doi.org/10.1016/j.bbamem.2020.183236
Received 23 December 2019; Received in revised form 14 February 2020; Accepted 25 February 2020
Available online 29 February 2020
0005-2736/

under physiologically-relevant conditions. Here, we feature the use of several biophysical methods, including solid-state NMR, to investigate the membrane interactions of copper-binding host defense peptides (HDPs) from the piscidin family. Bacterial membranes are battlegrounds for these peptides that can leverage multiple antimicrobial strategies such as copper-associated oxidative stress, structural and chemical modifications of phospholipids, and macrophage chemotaxis to sensitize biological membranes and achieve high antimicrobial efficacy [4–9]. However, the molecular mechanisms through which these peptides and other agents of the immune response could help synergize their antimicrobial effects at cell membranes remain elusive.

As the first line of defense against an infection or injury, the innate immune response is mediated by a variety of chemical species that orchestrate molecular recognition at the plasma membrane [4–7]. Initially, pathogenic cells are targeted by the constitutively produced proteins (e.g., HDPs) and phagocytic immune cells (e.g., neutrophils) that are recruited by signaling molecules and the complement system. Phagocytic cells generate and release reactive oxygen species (ROS) upon phagocytosis and stimulation by diverse agents [8,9]. ROS are involved in not only bacterial cell death, inflammation, and tissue injury, but also the activation of major signaling pathways [10–12].

HDPs feature evolution-tested efficacy against a broad spectrum of pathogens, including bacteria, fungi, yeasts, and viruses [13–17]. In spite of significant variations in sequence, length (6–50 residues) and sensitivity to changes in pH and ionic strength, they share physicochemical features (e.g., amphipathic secondary structures; cationicity). It is well accepted that the initial attraction and higher specificity of membrane-active HDPs for bacterial over mammalian cells is due to recognition of physicochemical properties of pathogenic cell membranes [18–25]. Properties that differ between bacterial and mammalian cells include surface charge (e.g.; anionic lipopolysaccharides or teichoic acids), composition (cholesterol content), fluidity, thickness, packing, and transmembrane potential.

Given the membrane affinity and activity of most HDPs, it is believed that they irreversibly disrupt pathogenic membranes by permeabilization (pores, defects) and/or disintegration (carpets). These mechanisms have been studied in model membranes by complementary methods (dye leakage assays, ion channel formation, CD, oriented CD (OCD) and NMR) [26–28]. The converging view for most HDPs is that at low peptide-to-lipid ratios (P/L), they acquire a surface-bound state ("S-state") but at increasing P/Ls they adopt a tilted state ("T-state") and cause leakage. However, details of their immunomodulatory effects, synergy with other immune molecules and access to intracellular components have recently emerged, leading to a new paradigm in which HDPs are thought to employ a multi-hit mechanism to directly eradicate bacteria and improve host immunity [13–16,29–35]. In keeping with their ability to target vital and ubiquitous parts of pathogenic cells (e.g. plasma membranes) through multi-hit mechanisms, they kill a broad range of not only dividing but also non-dividing pathogenic cells (e.g., planktonic; biofilm; persister) and have low incidence of resistance [35–39]. Thus, they represent promising templates for the development of novel therapeutics that are active against drug-resistant bacteria [40–43].

With the aim of better understanding the interplay between Cu^{2+} and HDPs as host defense agents at lipid membranes, we have been investigating copper-binding HDPs. More specifically, we speculate that the physicochemical properties of bacterial cell membranes and their surrounding environment produce conditions (e.g.; labile copper ions; ROS formation; anionic charge and oxidized lipid content of bilayers) that enable membrane-interacting host defense metallopeptides to develop membrane interactions conducive to membrane disruption. As explained next, several lines of evidence support this possibility.

Extensive research on biological copper ions shows that Cu^{2+} plays an essential role as an antimicrobial weapon [44]. "Macrophage copper burst" is part of the arsenal used by the phagolysosomes of macrophages to kill engulfed bacteria via a poisonous environment (low pH; high concentrations of copper, ROS and HDPs). The accumulated Cu^{2+} can attack bacteria by disrupting vital bacterial cuproenzymes and mediating Fenton chemical reactions that form toxic ROS [8,9].

Once formed, ROS have structural and functional implications for their surrounding environment, including bacterial cell membranes. ROS damage unsaturated fatty acids (UFAs) in phospholipid acyl chains, resulting in oxidized phospholipids (OxPLs) that exhibit double bond loss, a shortened acyl chain, and functionalization with aldehyde and hydroperoxy groups [45–47]. While lipid peroxidation has been investigated mainly in the context of mammalian cells and pathological conditions [48–52], it is also relevant to bacterial cells. For instance, some bacteria such as *Vibrio* species modulate their membrane properties and virulence by incorporating exogenous poly-UFAs (PUFAs) into their membranes [53–56].

Lipid oxidation affects model membranes, leading to: i) increased passive permeability; ii) modified phase behavior; iii) increased water content; iv) cross-linking between OxPLs and protein side chains [50,57–61]. These changes translate into disrupted membrane bulk properties, protein-lipid interactions, and thus altered biological function. Several HDPs (e.g., LL-37) experience enhanced interactions with bilayers containing zwitterionic 1- palmitoyl-2-(9′-oxo-nonanoyl)-*sn*-glycero-3-phosphocholine (commonly abbreviated as Aldo-PC or PoxnoPC, Fig. 1-A), an OxPL derived from the degradation of several UFAs. It contains an aldehyde group at the end of a shortened sn-2 acyl chain. High ionic strength mimicking in vivo conditions does not attenuate this effect even though it reduces peptide binding to anionic lipids [45,62].

Interestingly, several naturally-occurring HDPs, including piscidins from hybrid striped bass, have an amino terminal copper and nickel (ATCUN) binding motif (Fig. 1) [63–65]. As shown by our previous work, some of these peptides form a complex with labile Cu^{2+} that leads to ROS formation, lipid peroxidation, DNA damage, and enhanced biological activity [65–68]. Hence, ATCUN-HDPs can become metallated in the surrounding environment and adopt membrane-bound conformations that are favorable to the structural and chemical disruption of pathogenic cell membranes, and thus cell death. These results are captivating since they support the notion that ATCUN-HDPs could constitute a form of host defense through which several agents of the immune response integrate their anti-infective effects in multicellular organisms.

In this study, we focus on piscidin 1 (P1) (Fig. 1) as a membrane-interacting ATCUN-HDP that binds labile Cu^{2+} to enhance its antimicrobial effects. We use its homolog piscidin 3 (P3) for comparative purposes. Discovered in the mast cells of hybrid striped bass and later found in other teleost fish species (Fig. 1) [40,41,69–72], piscidins are histidine-rich HDPs that play a crucial defense role in fish fighting bacteria, viruses, and parasites [72]. Both the P1 and P3 forms have been functionally, structurally, and mechanistically investigated [73–78]. P1, the more antimicrobial, membrane-active, and hemolytic isoform, is less damaging to DNA than P3. With a minimum inhibitory concentration (MIC) <10 μM on most bacteria, it also has anti-cancer, anti-HIV-1, immunomodulatory and anesthetic properties [70,79–82]. This high potency together with other special features (e.g., resiliency to changes in ionic strength and pH changes [83], activation of immune cell chemotaxis [84]) makes P1 a unique template for the development of novel anti-infective therapeutics [40–43]. Mechanistically, the peptide deploys a multi-faceted strategy that includes exploiting heterogeneity in lipid bilayers containing certain lipid types, such as phosphatidylethanolamine (PE) and cholesterol [85]. These effects can directly impact membrane integrity or indirectly affect the function of membrane proteins (e.g., mechanosensitive channels) that interact with lipids.

Previous work has been useful in demonstrating that Cu^{2+} and Ni^{2+}

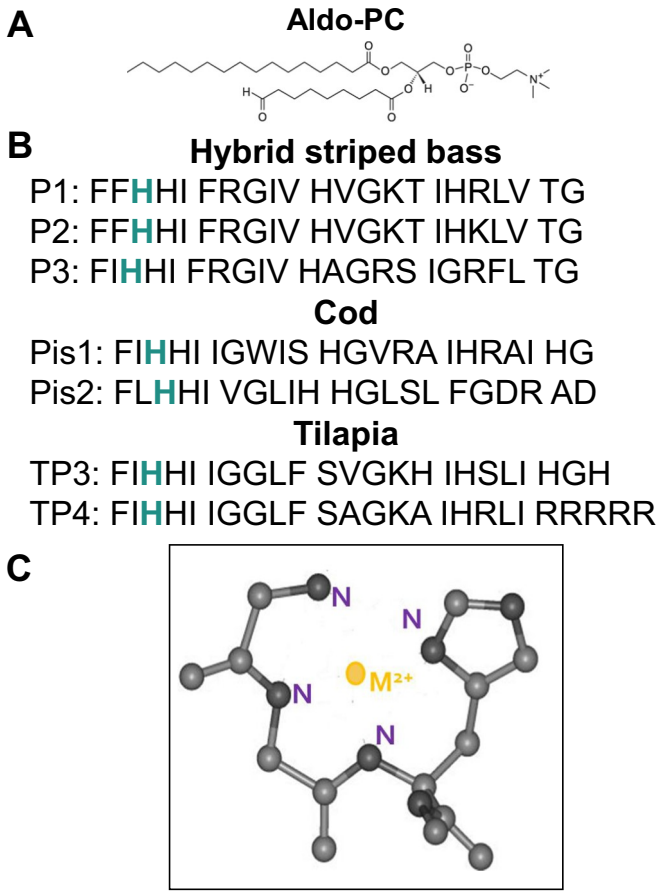

Fig. 1. Structures of the Oxidized Lipid of Interest and ATCUN Motif, and Sequences of Various Piscidins. (A) Structure of the oxidized lipid used in this study, AldoPC (obtained from Avanti Polar Lipids). (B) Amino acid sequences of piscidins found in hybrid striped bass, tilapia, and cod [40,41,69–72]. The conserved histidine at position 3 is highlighted in green. (C) Amino-terminal copper and nickel (ATCUN) Motif. The Motif ("XXH") includes three amino acids at the amino end of a protein chain, with the third amino acid being a histidine whose side chain is involved in metal coordination. The nitrogen atoms coordinating the metal are shown in purple and the metal ion, either Cu^{2+} or Ni^{2+}, appears in yellow.

bind specifically to the ATCUN motif of P1 and P3 in a 1:1 stoichiometric ratio, and that the ATCUN motif for piscidin is important for its antimicrobial effect [86,87]. However, there have been no characterizations on a molecular level of the impact that metallation has on its ability to permeabilize membranes and its interactions with different membrane constituents. Here, we start with dye leakage assays to study how metallation influences the membrane permeabilization effects of P1 with large unilamellar vesicles (LUVs). Next, we use circular dichroism (CD) to investigate whether Aldo-PC changes the binding affinity of P1 for bilayers. We used 10% Aldo-PC to reflect conditions that are expected to be physiologically relevant under oxidative stress [50,88]. We then turn to oriented-sample solid-state NMR to characterize how the peptide interacts with different lipid constituents and what topology it adopts in the bilayer. We focus on bacterial model membranes as a way to accurately and precisely control membrane composition and directly relate their molecular content to specific functional and conformational behaviors of the metallopeptides under native-like conditions, such as the presence of redox ions and OxPL. The knowledge gained from these studies provides new insight into structure-function relationships of piscidin, a good archetype of host defense metallopeptides that could be involved in combining the effects of antimicrobial agents.

2. Materials and methods

2.1. Materials, and peptide synthesis and verification

Chemicals were acquired from Fisher Scientific (Hampton, NH) unless otherwise indicated. The phospholipids were obtained from Avanti Polar Lipids (Alabaster, AL). ^{15}N-G13 P1 (MW 2572) and ^{15}N-G13 P3 (MW 2492) were synthesized using Fmoc-solid-phase peptide synthesis at the University of Texas Southwestern Medical Center (Dallas, TX). The peptides were purified by reverse phase HPLC on a Waters 150LC system fitted with a Waters XBridge C18 preparative column, as previously reported [73]. The mobile phases consisted of water and acetonitrile acidified with 0.1% trifluoroacetic acid (TFA). An acetonitrile/water gradient was run, allowing P1 and P3 to elute at ~30% acetonitrile [89]. The HPLC fractions containing pure peptide were lyophilized after removing the organic phase through rotatory evaporation. Next, the peptides were dissolved in dilute HCl (0.12 M) to substitute chloride for trifluoroacetate ions. After lyophilization, each peptide was dissolved in nanopure water and the pH adjusted to 7.4 prior to dialysis as needed to ensure the removal of any residual chloride ions. The solution collected at the end of dialysis was lyophilized and the dry powder dissolved in nanopure water. An aliquot of this solution was sent out for amino acid analysis (AAA) and concentration determination at the Protein Chemistry Lab at Texas A&M University (College Station, TX). Peptide purity was assessed to be 98% pure based on mass spectrometry and analytical HPLC [89].

2.2. ANTS/DPX leakage assays

Large unilamellar vesicles (LUVs) were prepared with the two different lipid compositions of 3.0:1.0 (molar) 1-palmitoyl-2-oleoyl-glycero-3-phosphocholine (POPC)/1-palmitoyl-2-oleoyl-sn-glycero-3-phosphoglycerol (POPG) and 2.6:1.0:0.40 (molar) POPC/POPG/1-palmitoyl-2-(9′-oxo-nonanoyl)-sn-glycero-3-phosphocholine (Aldo-PC). 5.1 μmol of lipids were dried from chloroform into a thin film in a glass vial under nitrogen gas, and then overnight under vacuum. The lipid was resuspended in 517 μl of degassed buffer at pH 7.0 containing 12.5 mM 8-aminonaphthalene-1,2,3-trisulfonic acid (ANTS), 45 mM *p*-xylylenebis(pyridinium bromide) (DPX), 10.0 mM sodium phosphate, and 100 mM potassium chloride. The lipid solutions were extruded 10 times using a 0.1 μm pore size Nuclepore polycarbonate filter (Whatman-GE Healthcare, Pittsburgh, PA). External ANTS and DPX were removed by gel filtration with Sephadex G100 (GE Healthcare, Pittsburgh, PA). Vesicle concentrations were measured by a modified Stewart Assay [90].

The lipid vesicles with entrapped ANTS and DPX were diluted with degassed pH 7 buffer containing only 10.0 mM sodium phosphate and 100 mM potassium chloride. The diluted vesicles were aliquoted into wells of a 96 well plate such that the final lipid concentration after addition of the peptide solution was 1.00 mM. The peptides P1 and P1−Cu^{2+} were added to the vesicles at P/L values of 1:256, 1:128, 1:64, 1:32, 1:16, 1:8, 1:4, and 1:2. Samples were prepared in triplicates. After 60 min, vesicle permeabilization was measured by an increase in ANTS fluorescence on a BioTek H4 Synergy Hybrid Microplate Reader, with excitation at 350 nm and emission at 519 nm. Fractional leakage was quantified using Eq. (1):

$$Fraction\ ANTS\ Leakage = \frac{I - I_{background}}{I_{triton} - I_{background}} \quad (1)$$

Here I is the intensity at 60 min, $I_{background}$ is the intensity of a control with vesicles only, and I_{triton} is the intensity in the presence of vesicles and 0.4% v/v of the detergent Triton X-100 added to completely permeabilize the vesicles and release the ANTS dye.

2.3. Circular dichroism-monitored titrations of large unilamellar vesicles with P1

Titration of P1 with PC/PG and PC/PG/Aldo-PC LUVs was followed by CD in phosphate buffer (3 mM, pH 7.4). LUVs were prepared as previously described [76]. Briefly, a lipid film was prepared in a round bottom flask by co-dissolving the lipids in chloroform. The solvent was evaporated under a flow of nitrogen gas prior to lyophilization overnight. Next, the lipid film was hydrated with buffer to yield a 5 mM lipid suspension. Following multiple freeze-thaw cycles, the suspension was extruded using an extruder at 100 nm for PC/PG and 200 nm for PC/PG/Aldo-PC. We note that the LUV size difference is not expected to affect the binding affinity since magainin-2, a similar HDP, gave rise to similar free energy of binding when 100 nm-LUVs and 30 nm-SUVs were used [91]. The LUVs were diluted to 2.00 mM prior to mixing with different amounts of peptide stock solution (283.8 and 232.5 μM for P1 in PC/PG and PC/PG/Aldo-PC) and buffer to yield P/L values varying between 0 and 80. Each sample was performed at fixed peptide concentration (20 μM). CD spectra for PC/PG and PC/PG/Aldo-PC were acquired at 298 K on a Jasco J-815 and J-1500 spectrometers (Jasco Analytical Instruments, Easton, MD), respectively, over a wavelength range of 190–260 nm using a scan speed of 100 nm/min, a 1 nm bandwidth, and four scans. For each P/L ratio, a blank containing the phosphate buffer and phospholipids but no peptide was obtained and subtracted from the piscidin signal to account for the background signal. Samples were made in duplicates using two different batches of LUVs yielding similar results. The molar ellipticity obtained at 222 nm was plotted in the form of a binding isotherm and fitted by a nonlinear least-squares minimization in Excel using the Solver Add-in to determine the dissociation constant, K_D.

2.4. Preparation of oriented samples for solid-state NMR

Oriented samples of P1, P1-Ni^{2+}, P3, and P3-Ni^{2+} were prepared using two different lipid mixtures: 3.0:1.0 (molar) POPC/POPG and 2.6:1.0:0.47 (molar) POPC/POPG/Aldo-PC. The peptides were reconstituted with the two lipid mixtures at molar P/L equal to either 1:80 or 1:20.

On day one of preparing a given sample, a lipid film containing 15 mg of lipids was made by co-dissolving the lipids in chloroform, evaporating the organic solvent under a flow of nitrogen gas, and lyophilizing overnight. For each sample, the amount of moles of peptide needed to reach a given P/L was obtained by pipetting from the aqueous peptide solution of concentration previously determined by AAA (typically on the order of 250 μM). Following lyophilization, the peptide powder was resuspended in 2.00 mL of nanopure water.

For samples containing P1 or P3 in the holo state, the 2.00-mL solution of peptide was titrated on day one with an equimolar amount of nickel chloride (Hampton Research, Aliso Viejo, California) to form the P1-Ni^{2+} or P3-Ni^{2+} complex, as previously reported [87]. The chloride form was used given that it is more physiologically relevant and divalent anions could affect membrane heterogeneity [92]. Because complex formation leads to deprotonation of the coordinating amine and amide bonds at the N-terminal end of the peptide, the pH dropped and had to be adjusted to 7.40 with NaOH. Due to the slow kinetics of metal binding to the ATCUN motif [93], the reaction takes a few minutes. Formation of the peptide-Ni^{2+} complex was readily visualized from the yellow color of the solution once the pH was sufficiently high. The presence of a stable complex was also verified by measuring UV–Vis spectroscopy since the ATCUN-Ni^{2+} complex absorbs light at 420 nm [94–96]. To be sure that the reaction with Ni^{2+} was complete, the samples were left overnight and the pH adjusted the next day if needed. On the second day, the lipid films were hydrated with the metallated peptide solution supplemented with 8.0 mL of BisTris buffer (3 mM, pH 7.4). The large amount of buffer ensured that the pH remained 7.4 in the final mixture.

For samples containing P1 or P3 in the apo state, the same steps were followed on the same time scale as for the holo peptides but nickel chloride was not added before adjusting the pH of the peptide solutions.

The hydrated lipid films were gently swirled to achieve complete mixing of the components. Incubation was carried out overnight at 40 °C prior to ultra-centrifugation on the third day at 8 °C for 1.5 h on a Beckman Optima-90 K centrifuge at 23,700 rpm (42,000 g, Beckman SW40Ti rotor). Next, the supernatant was pipetted out and stored at 4 °C while the pellet (~500–600 μl) was recovered and spread on 15–20 thin glass slides (dimensions 5.7 × 12 × 0.03 mm^3 from Matsunami Trading Co., Japan). The samples were then equilibrated in a closed chamber maintained at a relative humidity >90% using a saturated solution of K_2SO_4. This step usually took at least two days. Next, each slide was rehydrated by directly pipetting on it the quantity of corresponding supernatant necessary to reach 40% hydration by weight. The slides were then stacked and placed in a glass cell (internal dimensions 6 × 20 × 4 mm^3, Vitrocom Inc., NJ) prior to sealing with beeswax (Hampton Research, Aliso Viejo, CA) and incubating at 40 °C until appearing homogeneously hydrated, i.e. the samples were uniform in appearance and clear.

2.5. Solid-state NMR experiments

A low electric-field (*E*-field) HX flat coil probe [97] built by Black Fox (Tallahassee, FL) was employed to collect ^{31}P and ^{15}N chemical shifts on oriented samples studied above the phase transition of the lipids. This probe offered the benefit of preserving integrity of the hydrated samples during the high power solid-state NMR experiments [97,98].

2.5.1. ^{31}P solid-state NMR experiments

^{31}P solid-state NMR spectra were acquired under proton decoupling on the 750 Bruker Avance NMR spectrometer at William & Mary (W&M, Williamsburg, VA). Typical experimental parameters included a resonance frequency of 303.73 MHz, a 5.0-μsec 90° pulse on ^{31}P, and a proton decoupling power of 78 kHz. The temperature was equilibrated to 305 ± 0.1 K prior to recording 256 scans with a recycle delay of 3.0 s. All free induction decays were processed with 50 Hz of Gaussian line-broadening and the spectra referenced using an 85% aqueous solution of H_3PO_4 at 0 ppm. Given the overlapping resonances for the PC-rich and PG-rich regions, deconvolution of the spectra was considered. The lineshapes are Lorentzian and deconvolution did not affect the chemical shifts by >0.1 ppm. Thus, the reported chemical shifts were established using the original spectra.

2.5.2. ^{15}N NMR solid-state NMR experiments

^{15}N cross-polarization (CP) experiments were carried out at a resonance frequency of 76.03 MHz on the 750 MHz WB Bruker Avance NMR spectrometer at W&M. The probe used was the same as for the ^{31}P experiments (see above). Experimental parameters included a contact time of 1 msec, a CP field of ~ 50 kHz, a decoupling field of ~76 kHz, a recycle delay of 4.0 s, a temperature of 305 ± 0.1 K, and a number of transients equal to 1024. The ^{15}N data were processed with 50 Hz of Gaussian line-broadening and the spectra referenced to a saturated aqueous sample of $(^{15}NH_4)_2SO_4$, set at 26.8 ppm with respect to liquid NH_3.

3. Results

3.1. Dye leakage assays

To quantify the membrane permeabilization effects of P1 as a function of the lipid oxidation state and peptide metallation state, we measured the release of ANTS from LUVs made of either 3:1 POPC/POPG or 2.6:1:0.40 POPC/POPG/Aldo-PC following exposure to either P1 or P1-Cu^{2+}. Fig. 2 displays the fractional leakage from the LUVs as a

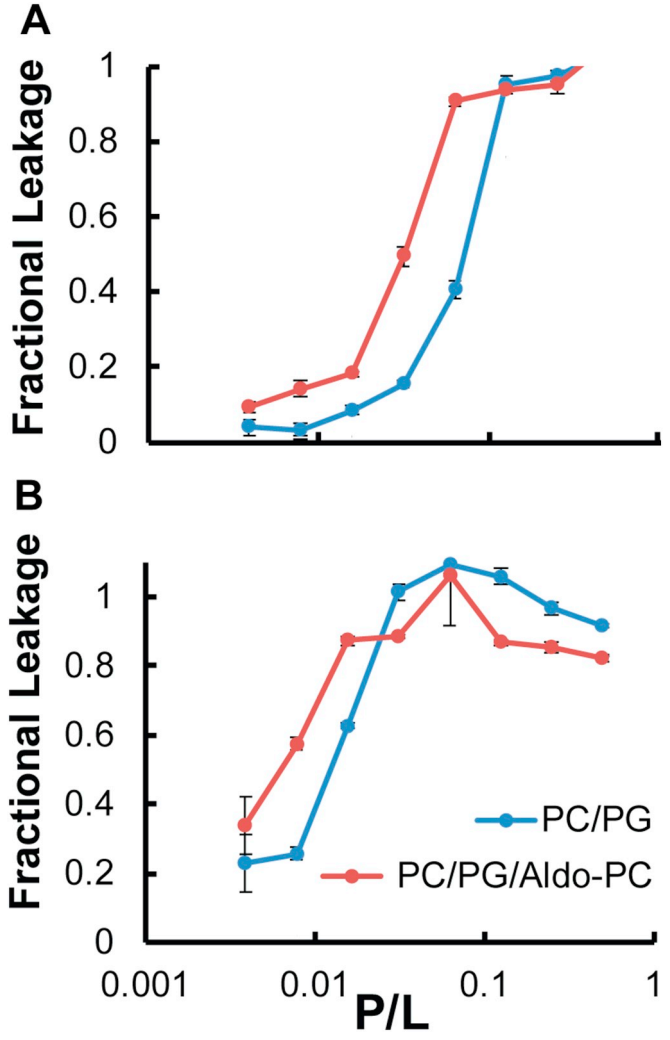

Fig. 2. Dye Leakage Assays for P1 and P1-Cu^{2+} Acting on PC/PG and PC/PG/Aldo-PC Vesicles. The fractional release (mean ± SD for triplicates) is displayed as a function of the peptide concentration. The tested conditions included 3:1 POPC/POPG (blue lines) and 2.6:1:0.4 POPC/POPG/Aldo-PC (red lines) LUVs exposed to P1 (A) and P1-Cu^{2+} (B).

Table 1
EC_{50} EC50 Values for Dye Leakage Assays of P1 and P1-Cu^{2+} in POPC/POPG and POPC/POPG/Aldo-PC.

$EC_{50values}$(P/L)	*PC/PG*	*PC/PG/ Aldo-PC*
P1	1:15	1:32
P1-Cu^{2+}	1:84	1:160

function of the P/L while Table 1 summarizes the EC_{50} values (effective concentration of peptide yielding 50% leakage) based on the response curves shown in Fig. 2. All curves are sigmoidal, in agreement with the permeation process being cooperative [99]. Both P1 and P1-Cu^{2+} induce leakage from the LUVs, but P1-Cu^{2+} is significantly more permeabilizing than P1, producing respective EC_{50} values of 1:84 and 1:15 in POPC/POPG. Furthermore, the effectiveness of P1 and P1-Cu^{2+} was doubled in the presence of Aldo-PC, yielding respective EC_{50} values of 1:32 and 1:160. Overall, these dye leakage results confirm the previously reported ability of P1 to be strongly permeabilizing [78,83,100–103]. Importantly, they demonstrate that the combination of metallating the peptide and the presence of OxPL increases its effectiveness by a factor of 10 compared to the apo-state in the PC/PG membrane (Fig. 2, Table 1).

In the P/L range where the peptide goes from inactive to membrane active, it is expected to transition from surface-bound (S-state) to inserted (I-state) [104,105]. Multiple factors influence the P/L at which a given peptide transitions from S- to I-state [28,106–109]. A major force driving the membrane binding and insertion of amphipathic peptides comes from the hydrophobic effect associated with the nonpolar side chains of the peptide. There may also be attractive forces between the cationic peptides and the phosphate group in the phospholipids. However, these favorable forces are not sufficient to overcome the cost of partitioning the polar peptide bonds at the water-bilayer interface unless secondary structure forms to hydrogen bond these polar groups.

When membranes contain anionic lipids, complex electrostatic effects between the HDP and lipids are also at play. On one hand, the anionic lipids attract the peptide to the bilayer surface until the lipid charge is neutralized by that of the bound peptides. On the other hand, this interaction tends to retain the peptide on the surface and hinder its ability to insert and adopt the disruptive I-state. Considering the electrostatic interactions on the membrane surface, full membrane lysis (100% leakage) will occur only if the forces driving insertion prevail, allowing the HDP to insert and interact cooperatively to permeabilize the bilayer before charge saturation takes place on the membrane and repulsive peptide-lipid electrostatics prevent more peptide molecules from binding to the membrane surface [110].

At pH 7.4, the charges of P1 and P1-Cu^{2+} predicted based on side chain pK_a values are Q = +4 and + 3, respectively, since the histidines are above their pK_a values; these were determined to be ≤6.0 in the presence of 3:1 PC/PG [83]. We note that Cu^{2+} binding to the ATCUN motif is accompanied by the loss of three protons, and thus the net loss of one positive charge from the peptide [86]. The predicted Q is expected to be higher than the effective charge experienced by the solvated peptide, i.e. $Q_{eff} < Q$ [111]. To a first approximation in our comparison of the two forms of the peptides, we will assume that the Q values apply here. In this case, each P1 molecule can neutralize four anionic PG headgroups. In a lipid mixture containing zwitterionic and anionic lipids mixed in a 3:1 M ratio, a quarter of the lipid molecules is anionic, and thus the PG headgroups will be neutralized by P1 at P1/L = 1:16. In the case of P1-Cu^{2+}, this value is P1-Cu^{2+}/L = 1:12. Thus, there is a modest advantage for P1-Cu^{2+} over P1 when we consider its ability to accumulate on bilayers before repulsive forces take place.

Based on the dye leakage assays (Fig. 2; Table 1), the plateau for about 100% leakage starts at P1/L = 1:8 and P1-Cu^{2+}/L = 1:16 in PC/PG; and P1/L = 1:32 and P1-Cu^{2+}/L = 1:64 in POPC/POPG/Aldo-PC. Given that P1 and P1-Cu^{2+} fully lyse all of the vesicles, both peptides have strong propensities for insertion and cooperative interaction. It is also true that the lower the peptide charge, the more effective a given form (P1 or P1-Cu^{2+}) is in a given lipid mixture. Thus, lower peptide charge correlates with enhanced membrane insertion and cooperative association. However, these considerations of charge do not explain why each peptide form is more active in the OxPL-containing membrane. In the next sections, we seek to address this question. We use CD and NMR to investigate on a molecular level the interactions of the two forms of the peptide with the different lipid components of the binary and tertiary lipid mixtures used in the dye leakage assays.

3.2. CD-monitored titrations of P1 with PC/PG and PC/PG/Aldo-PC LUVs

To determine whether Aldo-PC enhances the binding of P1 to bilayers, we used CD to titrate P1 into PC/PG and PC/PG/Aldo-PC vesicles. The peptide becomes α-helical upon LUV binding, while it is unstructured when it is not membrane bound (Fig. 3 and Fig. S1). The presence of a clear isosbestic point when the spectra for the titrations are stacked confirms that two states are present. Thus, we assumed that the α-helical content directly reports on membrane binding. Using the molar ellipticity at 222 nm as a reporter of α-helical content, binding isotherms were plotted and fitted to yield the dissociation constants

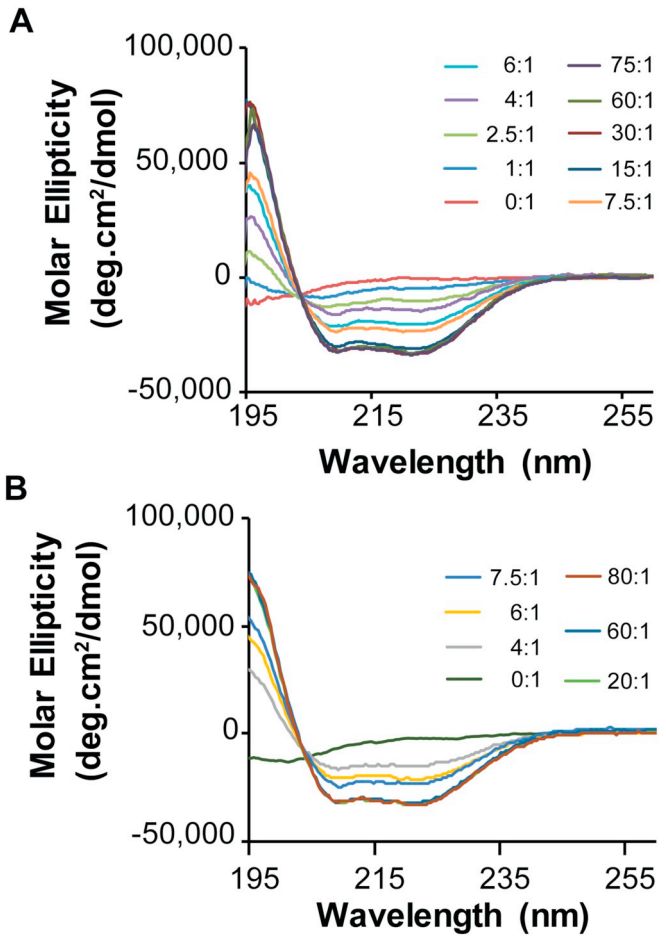

Fig. 3. CD-monitored Titrations of P1 with PC/PG and PC/PG/Aldo-PC LUVs. The titrations were done at a fixed concentration of peptide (20 μM) and varying amounts of 3:1 POPC/POPG (A) and 2.6:1:0.4 POPC/POPG/Aldo-PC (B) LUVs. Binding isotherms calculated from these titrations are shown in Fig. S1.

(Fig. S1). Similar K_D values on the order of 100 μM were obtained whether Aldo-PC was present or not. Thus, the two-fold improvement in permeabilization efficacy that P1 experiences when Aldo-PC is present cannot be explained based on stronger peptide-lipid interactions. Similar results were obtained with P3 (Fig. S2).

Because metal binding prevents the first few amino acids of the peptide from becoming α-helical, we did not test the metallated form of the peptide using CD-monitored titration. However, given that both the apo- and holo-states of P1 experience the same two-fold enhancement of membranolytic effects when Aldo-PC is available (Fig. 2, Table 1), an intrinsic property of the Aldo-PC membranes (rather than altered peptide-lipid interactions and mechanistic strategies associated with peptide metallation) must underlie the enhanced membrane disruption and the binding affinity is very likely not affected by metallation.

3.3. ^{31}P solid-state NMR experiments

3.3.1. Overview

As described above, the stronger membrane activity of piscidin in the OxPL-containing membranes cannot be fully explained by charge effects. Given that some cationic HDPs preferentially interact with anionic headgroups [112–116] and piscidin exploits heterogeneity in bilayers as part of its mechanism of membrane disruption [85], we speculated that the unmetallated and metallated peptide may interact differently with the multiple components of the bilayer, thereby enabling the metallated state to rearrange the lipids and form bilayer defects at a lower P/L threshold than possible with the apo-state. To gain more insight into this question, we performed ^{31}P solid-state NMR experiments on oriented samples prepared under conditions similar to those used for the dye leakage assays, i.e. using either metallated or unmetallated P1 interacting with either POPC/POPG or POPC/POPG/Aldo-PC bilayers. The headgroups of phospholipids act as "electrometers" that are highly sensitive to the presence of charged molecules in their proximity and ^{31}P oriented chemical shifts are excellent reporters of this effect [117–123]. Furthermore, there is a precedent for being able to resolve the ^{31}P resonances from PC and PG headgroups [120]. Based on all of these advantages of ^{31}P solid-state NMR, we used it to follow the POPC/AldoPC and POPG resonances in the presence of increasing amounts of metallated and unmetallated P1. We used Ni^{2+} to metallate the peptide in the NMR samples because it is diamagnetic when bound to the peptide. In contrast, Cu^{2+}, which remains paramagnetic when it is coordinated by the ATCUN motif, alters the relaxation properties of neighboring ^{31}P nuclei, leading to broad or vanished resonances, and thus preventing a straightforward interpretation of the signals [87]. Since both Ni^{2+} and Cu^{2+} generate similar planar structures of the ATCUN motif [124], using Ni^{2+} in the NMR experiments versus Cu^{2+} in the permeabilization assays is not expected to affect the peptide structure and partitioning behavior in membranes. We prepared the NMR samples at the P/L ratios of 1:80 and 1:20 to gain insight into the effects induced by the two states of the peptide in a concentration range where the permeabilization efficacy changes significantly, based on the data presented in Fig. 2 and Table 1.

Since ^{31}P is a spin-1/2 nucleus, its proton-decoupled spectra are dominated by the chemical shift interaction. This interaction is referred to as the chemical shift anisotropy (CSA) due to its angular dependence with respect to the static magnetic field, B_0 [126]. In the solution state, the fast and isotropic motions abolish the angular dependence and "isotropic" chemical shifts are observed. In the solid-state, as is the case for the mechanically-aligned extended bilayers used in this study, the CSA effect is observed, yielding anisotropic shifts [125,127,128].

The bottom spectra of Figs. 4 and 5 correspond to POPC/POPG and POPC/POPG/Aldo-PC oriented bilayers, respectively. In the absence of glass plates to align the samples and below the phase transition temperature of the lipids (T_m), the extended bilayers would be randomly oriented and in the gel state; thus the phospholipid molecules would give rise to a wide ^{31}P powder pattern spectrum, characterized by three discontinuities corresponding to σ_{11}, σ_{22}, and σ_{33}, the three principal components of the ^{31}P chemical shift tensor [126]. Above T_m, as is the case in our samples, these molecules rotate rapidly about their long axis, producing a motionally-averaged powder pattern that is axially symmetric and delineated by the tensor components $\sigma_\perp$ and $\sigma_{//}$. The former correlates to molecules oriented with their long axis perpendicular to B_0 while the latter corresponds to a parallel orientation of the lipid molecules and B_0. When the phospholipid molecules are mechanically oriented on glass plates and the samples placed in the NMR probe so that the bilayer normal is parallel to B_0, only the chemical shift at $\sigma_{//}$ persists near 25–30 ppm [120]. Edge effects due to the mosaic spread can lead to a small amount of signal at $\sigma_\perp$ (~ -15 ppm) [129].

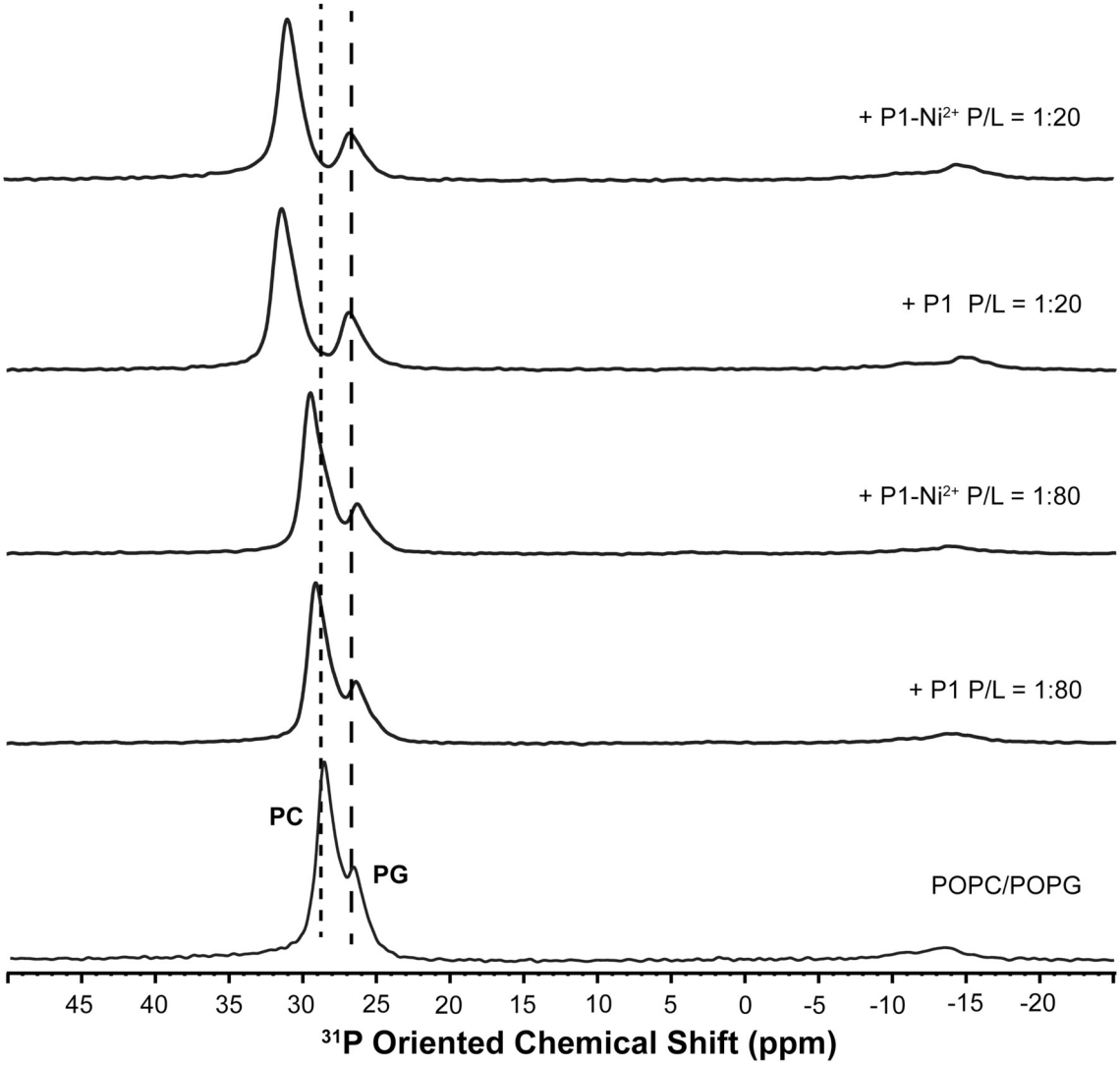

Fig. 4. ^{31}P Solid-state NMR Spectra of PC/PG in the presence of P1 and P1-Ni^{2+}. ^{31}P chemical shifts were collected at 305 K under proton decoupling. The samples were analyzed so that the bilayer normal was parallel to the static magnetic field, B_0. The displayed spectra correspond to 3:1 POPC/POPG hydrated bilayers studied in the absence or presence of P1 or P1-Ni^{2+} at P/L = 1:80 and 1:20, as indicated. Vertical lines indicate the positions of the PC- (short dashes) and PG- (long dashes) regions in neat POPC/POPG. Labels on the lipid-only sample indicate the positions of the PC and PG resonances. Table 2 lists the chemical shift data extracted from these spectra.

3.3.2. Effects of P1 and P1-Ni^{2+} on POPC/POPG and POPC/POPG/Aldo-PC bilayers

Taking a closer look at the spectra shown in Figs. 4 and 5 for POPC/POPG (binary mixture) and POPC/POPG/Aldo-PC (tertiary mixture), respectively, the strong oriented shifts around 25–30 ppm indicate that the phospholipid molecules are well oriented. A small amount of signal around −15 ppm corresponds to unoriented bilayers due to the mosaic spread. Upon examination of the signal near 25–30 ppm, two resonances are observed, as expected from samples containing two types of lipid headgroups. In agreement with previously published spectra of PC/PG bilayers (reviewed in [120]) and consistent with the 3:1 M ratio, the downfield resonance at 28.8 ppm corresponds to the PC headgroup while that at 26.8 ppm arises from the PG lipid. The single peak observed for the PC region indicates that POPC and Aldo-PC are indistinguishable in terms of ^{31}P oriented signal. This is consistent with previous ^{31}P data obtained with Aldo-PC studied in unoriented bilayers by static and magic angle techniques [58].

Histograms plotted in Fig. 6 help visualize the changes experienced by the ^{31}P chemical shifts as different parameters, including metallation of P1 and the addition of OxPL, are varied in the samples (Tables 2 and 3). Upon addition of P1 (blue, Fig. 6) and P1-Ni^{2+} (green, Fig. 6) to 3:1 POPC/POPG at P/L = 1:80, the changes are very small. However, at P/L = 1:20, the PC resonance is strongly affected by the peptide, becoming broader and moving downfield, which indicates an increase in the ^{31}P CSA and the reorientation of these lipid headgroups. This effect was previously observed for other membrane-binding molecules [117,118,130]. Thus, both forms of the peptide accumulate strongly near the PC headgroups. These trends were confirmed by making duplicate samples as well as by studying the effects of P3 and P3-Ni^{2+} on the binary and tertiary lipid mixtures (Figs. S3 and S5).

Remarkably, the PG-rich region is highly sensitive to the metallation state of the peptide and OxPL content. As seen in Fig. 6, ΔCS(PG) at P/L = 1:20 is only 0.1 ppm in the PC/PG/P1 sample while it is 3.0 ppm in the PC/PG/Aldo-PC/P1-Ni^{2+} counterpart. In contrast, ΔCS(PC) is quite similar under these two sets of conditions. Thus, the PG headgroup region responds more strongly to the presence of the peptide when the peptide is metallated and the OxPL is present.

Overall, the ^{31}P NMR data demonstrate that in the presence of OxPL, the metallated peptide interacts more readily with the PG region. Importantly, the strong interaction of P1-Ni^{2+} with the anionic lipid

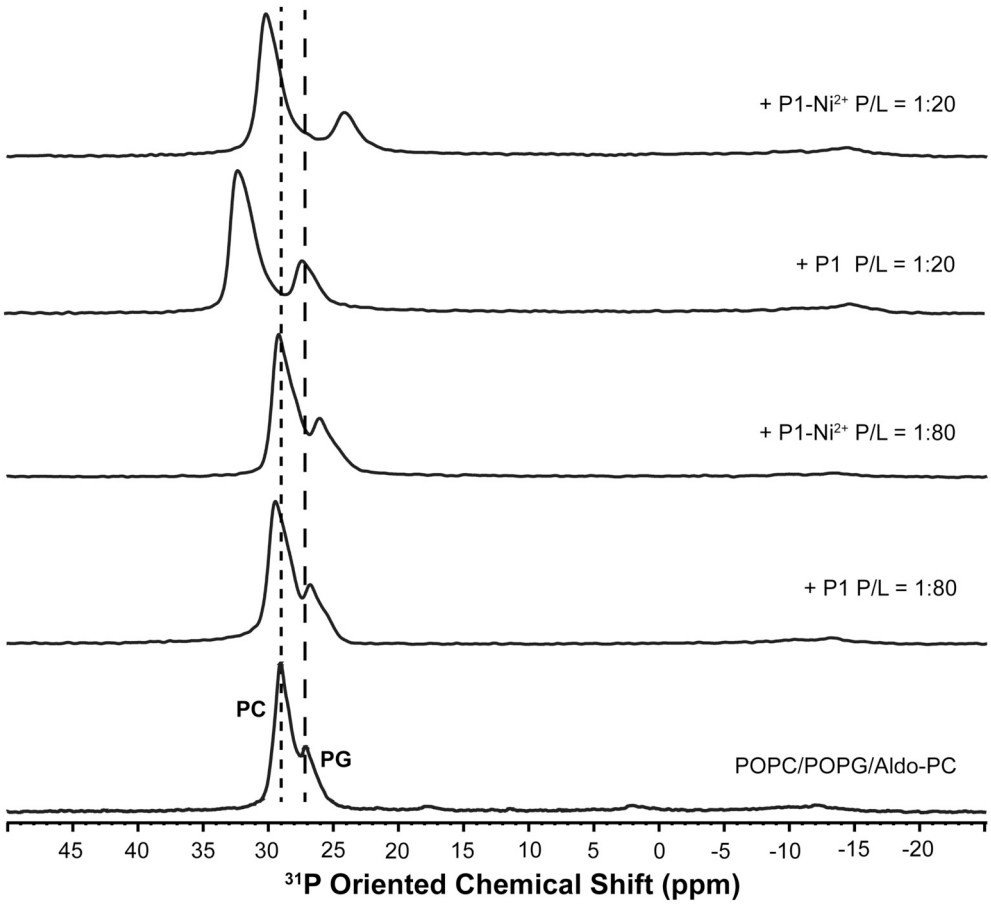

Fig. 5. ^{31}P Solid-state NMR Spectra of PC/PG/Aldo-PC in the presence of P1 and P1-Ni^{2+}. ^{31}P chemical shifts were collected at 305 K under proton decoupling. The samples were analyzed so that the bilayer normal was parallel to the static magnetic field, B_0. The displayed spectra correspond to 2.6:1:0.47 POPC/POPG/Aldo-PC hydrated bilayers studied in the absence or presence of P1 or P1-Ni^{2+} at P/L = 1:80 and 1:20, as indicated. Vertical lines indicate the positions of the PC- (short dashes) and PG- (long dashes) regions in neat POPC/POPG/Aldo-PC. Labels on the lipid-only sample indicate the positions of the PC and PG resonances. Table 3 lists the chemical shift data extracted from these spectra.

Table 2
^{31}P Chemical Shift Data for POPC/POPG in the Presence of P1 and P1-Ni^{2+}.[a]

^{31}P chemical shifts (ppm)	PC - region	PG - region
PC/PG	28.8	26.8
+ P1 (1:80)	29.1	26.4
+ P1-Ni^{2+} (1:80)	29.4	26.3
+ P1 (1:20)	31.4	26.9
+ P1-Ni^{2+} (1:20)	30.9	26.7

[a] The error bar is ±1 ppm based on replicates (see Methods).

Table 3
^{31}P Chemical Shift Data for POPC/POPG/Aldo-PC in the Presence of P1 and P1-Ni^{2+}.[a]

^{31}P chemical shifts (ppm)	PC - region	PG - region
PC/PG/Aldo-PC	29.0	27.1
+ P1 (1:80)	29.5	26.8
+ P1-Ni^{2+} (1:80)	29.2	26.2
+ P1 (1:20)	32.2	27.2
+ P1-Ni^{2+} (1:20)	30.2	24.1

[a] The error bar is ±1 ppm based on replicates (see Methods).

component only when the OxPL is present correlates well with the stronger membrane activity of the metallated peptide on the tertiary lipid mixture (Fig. 2, Table 1). The results also show that the simple addition of 10% OxPL to the membrane sensitizes it to the action of the apo-peptide without changing its affinity for the PC and PG membrane components. Thus, a property intrinsic to the OxPL-containing membrane is implicated in the enhanced membrane activity.

3.3.3. Effects of free Ni^{2+} on POPC/POPG and POPC/POPG/AldoPC bilayers

We performed complementary experiments where we added free Ni^{2+} in molar amounts equal to that of P1-Ni^{2+} in the P/L = 1:20 samples. Importantly, free Ni^{2+} is paramagnetic due to its octahedral geometry in coordination with water [$Ni(H_2O)_6$] while Ni^{2+} coordinated to the ATCUN motif is in a square planar geometry and diamagnetic [93]. Thus, the experiments with free Ni^{2+} feature complex relaxation effects that are absent in the P1-Ni^{2+} samples. Nevertheless, they provide some insight into any preferential partitioning that may occur when the divalent cation is present.

As shown in Fig. S6, the addition of Ni^{2+} at the molar equivalent of P/L = 1:20 to the binary lipid mixture dramatically affects the chemical shifts of both the PC and PG resonances by moving them upfield. Both the chemical shift value and intensity of the PG resonance are affected. The change in chemical shift can be explained by the preferential binding of the cation to the anionic lipid while the decrease in signal strength is attributed to the interactions of the paramagnetic center with the ^{31}P nuclei in the PG headgroups. Notably, adding P1-Ni^{2+} to bilayers leads to a change in chemical shift but not intensity of the PG resonance. This confirms that Ni^{2+} is diamagnetic bound to the peptide and no free Ni^{2+} is present. This is because we carefully added stoichiometric amounts of metal ion to the peptide and the peptide-metal interaction is very strong [86]

Interestingly, the intensity of the PG resonance is not affected as much by free Ni^{2+} when the OxPL is present. This suggests that Ni^{2+} does not have as much access to the PG headgroup as it does in the binary lipid mixture. This is consistent with the reorientation of the sn-2 chain to reach the lipid-water interface that was detected in MD simulations of bilayers containing 25% Aldo-PC [59]. The layering of the aldehyde group of the acyl chain on the surface of the bilayer may prevent the Ni^{2+} from approaching the PG phosphate group.

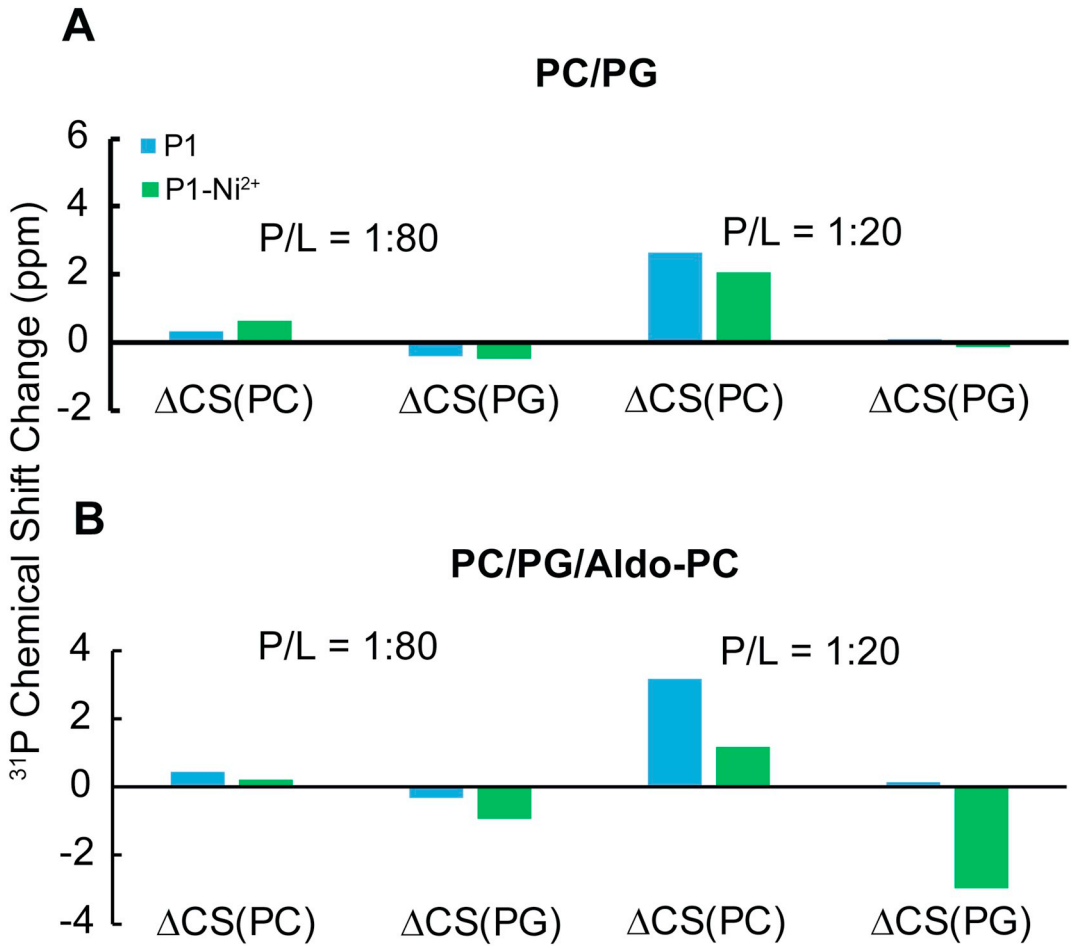

Fig. 6. ^{31}P Chemical Shift Changes for POPC/POPG and POPC/POPG/Aldo-PC in the Presence of P1 and P1-Ni^{2+}. The chemical shift changes are indicated for the PC-(ΔCS(PC)) and PG- regions (ΔCS(PG)) for POPC/POPG (A) and POPC/POPG/Aldo-PC (B) exposed to P1 (blue) and P1-Ni^{2+} (green) at P/L = 1:80 and 1:20.

3.4. ^{15}N solid-state NMR experiments

We investigated the orientation of P1 and P1-Ni^{2+} in the binary and tertiary lipid mixture using ^{15}N NMR cross-polarization experiments. Using the same oriented samples as for the ^{31}P studies, we detected the signal of ^{15}N-G13-P1 and ^{15}N-G13-P1-Ni^{2+} at P/L = 1:20. G13 lies in the center of the α-helical region of the peptide, a region remote from the metal-binding site. As illustrated in Fig. 7, all samples gave rise to a sharp resonance near 62 ppm. Similar to the oriented ^{31}P chemical shifts, this value reports on the molecular orientation of the α-helical peptide with respect to B_0. Being close to σ_{11} and σ_{22}, this chemical shift is consistent with the α-helical part of the peptide orienting its long axis almost parallel to the membrane surface [131–133]. Given the similarity of the different spectra in Fig. 7, the orientation of the α-helical part of the peptide with respect to the bilayer surface is affected by neither the presence of OxPL nor peptide metallation. However, significant broadening of the resonance occurs when the OxPL is present and metallated state of the peptide is used as shown in Table S3, suggesting that the peptide adopts a broader range of orientations in the tertiary mixture. As discussed below, this result together with the strong PG/P1-Ni^{2+} interaction detected by ^{31}P NMR is consistent with the possible formation of multiple domains, such as PC-rich and PG-rich regions, that could destabilize the membrane and explain the particularly strong disruptive effects achieved by metallated P1 in the tertiary lipid mixture.

4. Discussion

This study lies at the interface of several areas of research: the mechanism of action of HDPs, the possible synergistic effects between antimicrobial agents, and the impact of OxPLs on lipid-protein interactions. More specifically, we have explored the novel paradigm that copper-binding HDPs could represent an interesting form of host defense that unifies the effects of several antimicrobial agents available at lipid membranes. Not only does metal-binding provide these HDPs with an opportunity to alter their charge state, but it also places a redox center in the membrane, as needed to form ROS in proximity to the double bonds of UFAs. While ROS formation is faster for free Cu^{2+} [86], the coordination to a cationic peptide provides enhanced specificity to negatively-charged microbial membranes. Oxidized lipids alter the structural arrangement of membranes [50,57–61]. To our knowledge, we provide the first example of oriented sample solid-state NMR applied to bilayers containing OxPLs. Together, our NMR, CD, and dye leakage experiments on the apo- and holo-forms of P1 in OxPL-containing membranes demonstrate that both peptide metallation and OxPL availability significantly enhance the membrane disruptive effects of the peptide. Next, we discuss how metallation and OxPL availability could produce this outcome.

We previously showed that the metallation of piscidin improves its antimicrobial effects and results in significant lipid peroxidation [86]. Here, our finding that both peptide metallation and OxPL availability enhance membrane activity provides a starting point to explain on a

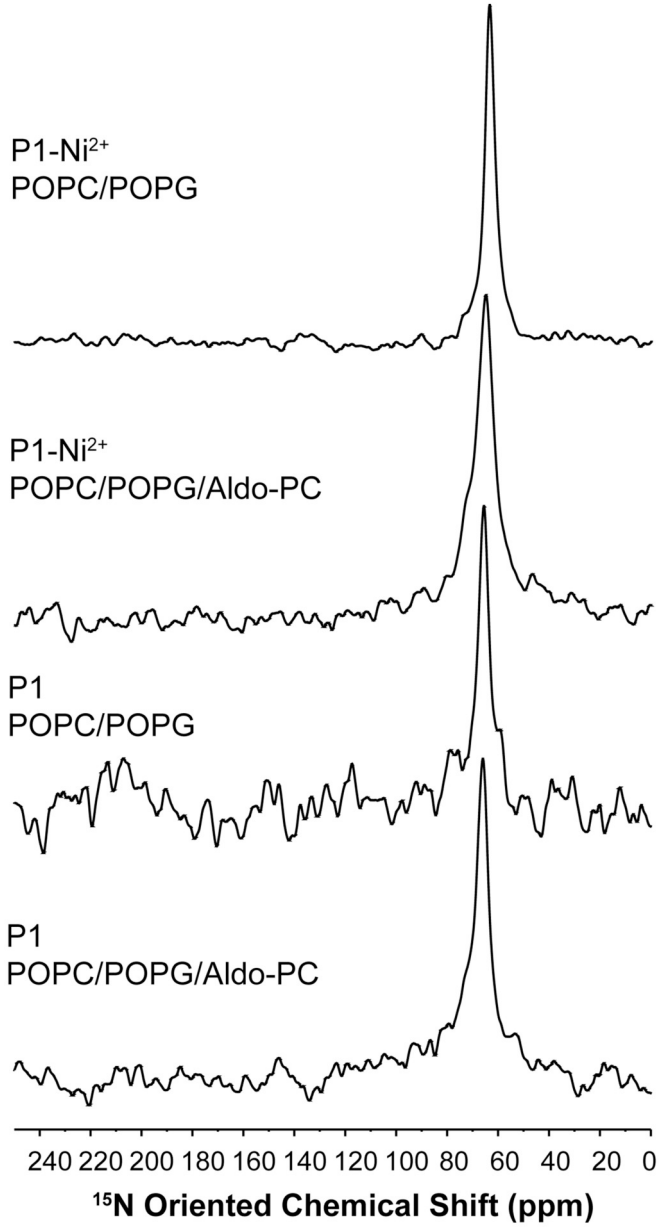

Fig. 7. ^{15}N Chemical Shift Spectra for ^{15}N-G13 P1 and ^{15}N-G13 P1-Ni^{2+} Bound to Aligned POPC/POPG or POPC/POPG/Aldo-PC Bilayers. These oriented sample solid-state NMR spectra were collected at 305 K under cross polarization using samples prepared at P/L = 1:20. The signal of ^{15}N-G13, which is in the α-helical region of the peptide whether the ATCUN motif is metallated or not, is observed at about 62 ppm. This is consistent with an orientation of the peptide parallel to the bilayer normal. Full widths at half-height are given in Table S3.

molecular level the biological effects of metallation (e.g.; lower MICs and enhanced lipid peroxidation) and supports the notion that copper-binding peptides can help integrate the activities of antimicrobial agents. Importantly, free Cu^{2+} is antimicrobial but lacks specificity. Thus, its association with a membrane-binding HDP provides the advantage of bringing this redox center to pathogenic cell membranes with more specificity than possible with labile Cu^{2+}. Zn^{2+} is another ubiquitous metal ion that has been involved in boosting the activity of some HDPs through motifs such as HEXXH (e.g., histatin-5) and HXXXH (e.g., clavanin A) [64,134]. However, P1 does not feature these motifs.

In terms of mechanism of action, our earlier work on the apo-state in model membranes containing either PE or PC combined with PG points at the formation of transient defects rather than toroidal pores to explain membrane permeation [83,85,135]. As shown in our current study, metallation of P1 leads to the same five-fold enhancement of membranolysis whether PC/PG or PC/PG/Aldo-PC LUVs are used. Thus, metallation provides an advantage that is intrinsic to P1. Conversely, making Aldo-PC available results in the same two-fold enhancement whether the apo- or holo-state is used. Hence, a property intrinsic to the OxPL-containing bilayer is responsible for the enhanced membrane activity by both forms of the peptide.

Previous studies of HDPs showed that OxPL can enhance the affinity of the peptide for bilayers [45,50]. This was explained by the reversal of the sn-2 chain, which makes it orient almost perpendicular to the bilayer normal at the water-bilayer interface. Such exposure of the polar sn-2 chain on the surface of the membrane was postulated to represent binding sites for HDPs. From our CD data, we did not find that P1 bound bilayers more readily when Aldo-PC was present. This is consistent with the changes in ^{31}P chemical shifts of the PC-headgroup region not being stronger in the Aldo-PC containing samples when P1 is added (Fig. 5). Thus, we conclude that the oxidized chain of Aldo-PC is not targeted by piscidin.

With regard to the physical changes occurring in bilayers upon the addition of OxPL, earlier ^{31}P NMR studies of unoriented samples by the group of Gröbner showed that adding Aldo-PC to 1,2-dimyristoylphosphatidylcholine (DMPC) leads to phase separation below and near the phase transition of the lipids [58]. Based on differential scanning calorimetric (DSC) data, up to three domains were detected while ^{2}H NMR experiments showed a significant increase in headgroup hydration in the presence of Aldo-PC. Above the phase transition, fast exchange between domains results in fluid and homogeneous membranes. However, molecular dynamics (MD) simulations showed that bilayers in the fluid state are thinner when Aldo-PC is present [59]. These studies show that Aldo-PC has a propensity to induce domain formation and thinning in an otherwise well behaved phospholipid bilayer. Clearly, membrane thinning and increased hydration of bilayers in the presence of Aldo-PC would help piscidin form leakage-competent defects across the membrane. Furthermore, domain boundaries may represent a targeted site of action of membrane-active peptides [136].

Interestingly, we recently demonstrated that P1 exploits heterogeneity in membranes containing either PE or cholesterol, and that these effects correlate with its ability to lower the activation threshold for mechanosensitive channels from *E. coli* [85]. In cholesterol-containing membranes, P1 induces phase separation, leading to liquid-ordered (L_o) and liquid-disordered (L_d) domains.

Peptide binding to phospholipid bilayers can affect the ^{31}P chemical shifts of the headgroups directly or indirectly [117,125,133]. First, the binding of the peptide in the lipid headgroup region can directly alter the conformations and chemical environment of the headgroups. Second, the peptide can bind in a way that changes the overall bilayer structure, resulting in changes in the arrangement and chemical environment of the headgroups. Our NMR data indicate that in PC/PG, both P1 and P1-Ni^{2+} impact only the ^{31}P chemical shifts of the PC headgroups, indicating that the peptide directly interacts or indirectly alters this component of the bilayer. In contrast, when the OxPL is present, P1-Ni^{2+}, but not P1, dramatically influences the ^{31}P chemical shift of the PG headgroups. Therefore, the specificity of the peptide to directly or indirectly affect a given lipid component is dependent on not only its metallation state but also whether the structurally-disruptive lipid is present or not. The strong specificity for one lipid type suggests that in a fashion similar to its effect in PC/Cholesterol bilayers, the peptide prefers binding to one lipid type, promoting the formation of PC- and PG-rich domains, and yielding boundary sites that may be more susceptible to membrane attack compared to well mixed bilayers. As shown by comparing the data collected at P/L = 1:80 and 1:20, when the PG region becomes saturated at the higher P/L, the peptide also interacts with the PC region. If domain formation plays a role in the mechanism of membrane disruption by P1, we would expect it to contribute similarly in PC/PG versus PC/PG/Aldo-PC or for the apo-

versus holo-states since the improvement in permeabilization is conserved when one of these parameters (metallation, lipid content) is changed and the other kept constant. While there may not be a mechanistic advantage to having P1-Ni^{2+} interact preferentially with PG, this acquired specificity could be advantageous in vivo, as further discussed below.

With regard to properties intrinsic to P1 that could underlie the five-fold improvement in membrane activity upon metallation, both the charge and the structure of the peptide are altered by metal binding, and both could explain enhanced membrane activity. Indeed, the lower charge and flatter shape of the amino terminal end achieved upon metal coordination of the ATCUN motif could indeed promote the insertion of the peptide in the bilayer. From this perspective, the partitioning of the irregularly-structured metallated peptide in a bilayer that is structurally rearranged and thinned due to OxPL would explain its particularly strong membrane disruptive effects in PC/PG/Aldo-PC. It is also possible that metallation of the amino terminal is conducive to oligomer formation and enhanced bilayer disruption, a situation previously reported for the amyloid-beta peptide [137].

Given that the apo-state of P1 is fully α-helical [73] and its affinity for PC is not affected by the addition of Aldo-PC, while the holo-state adopts a square planar geometry at its amino end and is strongly attracted to PG in the presence of Aldo-PC, we conclude that the irregular conformation of P1-Ni^{2+} directs it to the PG headgroups, leading to a PG-rich region that is rich in peptide but depleted in PC headgroups. We speculate that the reorientation of the sn2-acyl chain of Aldo-PC to the bilayer interface leads to a structural organization of the bilayer that is not conducive to the partitioning of the irregularly structured metallated peptide in the PC headgroups.

It is interesting that free Ni^{2+} interacts strongly with PG in PC/PG, but not when OxPL is present. In drastic contrast, P1-Ni^{2+} preferentially interacts with PG in the tertiary lipid mixture. Thus, even if metallation leads to the same five-fold improvement of permeabilization effects whether Aldo-PC is present or not, the specifics of the underlying interactions are different depending on the metallation state. Remarkably, the peptide-metal complex is more specific to the anionic content of bacterial membranes when Aldo-PC is present. In the context of in vivo conditions, this could have important implications since the peptide is expected to be secreted in the holo-state [86] and concomitantly to the release of ROS by phagocytic cells [138]. Given the formation of OxPLs by ROS and the fact that the metallated state of the peptide is the more membrane-active form, the peptide could be more specifically directed to the anionic lipids that differentiate pathogenic from healthy (host) cells.

5. Conclusions

In conclusion, these studies of P1 as an ATCUN-containing HDP demonstrate that metallation of HDPs could represent an interesting pathway used in nature to unify how membrane-interacting antimicrobial agents achieve their effects. It also provides new molecular-level insight into the roles that OxPLs play in the efficacy of membrane-active peptides. In particular, it is fascinating that the membrane-activity of the peptide and its specificity for the anionic lipids characteristic of pathogenic cell membrane surfaces are simultaneously optimized when the peptide is metallated and OxPLs are available. The methods used here could be useful to study other peptides and proteins that interact with OxPLs. We hope that this work will stimulate further studies to better understand the biological effects of metal-binding peptides and oxidized lipids.

Declaration of competing interest

The authors declare that they have no known competing financial interests or personal relationships that could have appeared to influence the work reported in this paper.

Acknowledgements

MLC acknowledges support from the National Science Foundation (MCB-1716608), Research Corporation for the Advancement of Science, and the Camille and Henry Dreyfus Foundation. KH thanks the National Science Foundation (DMR 1709892) for support. The authors recognize Cotten group members who helped purify piscidin peptides. MLC acknowledges the significant contributions, inspiration, and support that Prof. Michèle Auger provided to the international biological solid-state NMR community. She will be greatly missed.

Author contributions

MLC conceptualized and administered the project, obtained funding and identified resources, supervised team members at William & Mary, performed CD and NMR experiments, analyzed and interpreted the CD, NMR, and dye leakage data, made the figures, and wrote and edited the manuscript. SP purified peptides, made the majority of the samples for ^{31}P and ^{15}N NMR, ran some of the NMR experiments, and organized some of the ^{31}P NMR results for publication. AIG performed NMR experiments and fitted the binding isotherms. MR made some of the duplicate samples for ^{31}P NMR. SK designed and performed the dye leakage experiments at Johns Hopkins University, with KH providing the resources. All co-authors read the manuscript and provided feedback.

Appendix A. Supplementary data

Supplementary data to this article can be found online at https://doi.org/10.1016/j.bbamem.2020.183236.

References

[1] D.M. Engelman, Membranes are more mosaic than fluid, Nature 438 (2005) 578–580.
[2] J. Lombard, Once upon a time the cell membranes: 175 years of cell boundary research, Biol. Direct 9 (2014) 32.
[3] U. Coskun, K. Simons, Cell membranes: the lipid perspective, Structure 19 (2011) 1543–1548.
[4] E. Meylan, J. Tschopp, M. Karin, Intracellular pattern recognition receptors in the host response, Nature 442 (2006) 39–44.
[5] B. Pulendran, K. Palucka, J. Banchereau, Sensing pathogens and tuning immune responses, Science 293 (2001) 253–256.
[6] S. Joyce, Immune recognition, response, and regulation: how T lymphocytes do it, Immunol. Res. 23 (2001) 215–228.
[7] A. Aderem, R.J. Ulevitch, Toll-like receptors in the induction of the innate immune response, Nature 406 (2000) 782–787.
[8] J.M. Slauch, How does the oxidative burst of macrophages kill bacteria? Still an open question, Mol. Microbiol. 80 (2011) 580–583.
[9] A.N. Besold, E.M. Culbertson, V.C. Culotta, The Yin and Yang of copper during infection, J. Biol. Inorg. Chem. 21 (2016) 137–144.
[10] C. Kohchi, H. Inagawa, T. Nishizawa, G. Soma, ROS and innate immunity, Anticancer Res. 29 (2009) 817–821.
[11] X. Chen, M. Song, B. Zhang, Y. Zhang, Reactive oxygen species regulate T cell immune response in the tumor microenvironment, Oxidative Med. Cell. Longev. 2016 (2016) 1580967.
[12] W. Dröge, Free radicals in the physiological control of cell function, Physiol. Rev. 82 (2002) 47–95.
[13] T. Ganz, R.I. Lehrer, Antimicrobial peptides of vertebrates, Curr. Opin. Immun. 10 (1998) 41–44.
[14] R.M. Epand, H.J. Vogel, Diversity of antimicrobial peptides and their mechanisms of action, Biochim. Biophys. Acta 1462 (1999) 11–28.
[15] T. Ganz, R.I. Lehrer, Antibiotic peptides from higher eukaryotes: biology and applications, Mol. Med. Today 5 (1999) 292–297.
[16] A. Koczulla, R. Bals, Antimicrobial peptides: current status and therapeutic potential, Drugs 63 (2003) 389–406.
[17] A. Patrzykat, S. Douglas, Antimicrobial peptides: cooperative approaches to protection, Protein Pept Lett. 12 (2005) 19–25.
[18] J.D. Lear, Z.R. Wasserman, W.F. DeGrado, Synthetic amphiphilic peptide models for protein ion channels, Science 240 (1988) 1177–1181.
[19] Y. Agawa, S. Lee, S. Ono, H. Aoyagi, M. Ohno, T. Taniguchi, K. Anzai, Y. Kirino, Interaction with phospholipid bilayers, ion channel formation, and antimicrobial activity of basic amphipathic alpha-helical model peptides of various chain

lengths, J. Biol. Chem. 266 (1991) 20218–20222.
[20] M. Dathe, M. Schumann, T. Wieprecht, A. Winkler, M. Beyermann, E. Krause, K. Matsuzaki, O. Murase, M. Bienert, Peptide helicity and membrane surface charge modulate the balance of electrostatic and hydrophobic interactions with lipid bilayers and biological membranes, Biochemistry 35 (1996) 12612–12622.
[21] Y. Shai, Mechanism of the binding, insertion and destabilization of phospholipid bilayer membranes by alpha-helical antimicrobial and cell non-selective membrane-lytic peptides, Biochim. Biophys. Acta 1462 (1999) 55–70.
[22] N. Sitaram, R. Nagaraj, Interaction of antimicrobial peptides with biological and model membranes: structural and charge requirements for activity, Biochim. Biophys. Acta 1462 (1999) 29–54.
[23] M. Dathe, H. Nikolenko, J. Meyer, M. Beyermann, M. Bienert, Optimization of the antimicrobial activity of magainin peptides by modification of charge, FEBS Lett. 501 (2001) 146–150.
[24] R.E.W. Hancock, A. Rozek, Role of membranes in the activities of antimicrobial cationic peptides, FEMS Microbiol. Lett. 206 (2002) 143–149.
[25] Y. Shai, Mode of action of membrane active antimicrobial peptides, Biopolymers 66 (2002) 236–248.
[26] M.-T. Lee, W.-C. Hung, F.-Y. Chen, H.W. Huang, Mechanism and kinetics of pore formation in membranes by water-soluble amphipathic peptides, Proc. Natl. Acad. Sci. U. S. A. 105 (2008) 5087–5092.
[27] B. Bechinger, K. Lohner, Detergent-like actions of linear amphipathic cationic antimicrobial peptides, Biochim. Biophys. Acta Biomembr. 1758 (2006) 1529–1539.
[28] W.C. Wimley, Describing the mechanism of antimicrobial peptide action with the interfacial activity model, ACS Chem. Biol. 5 (2010) 905–917.
[29] K.A. Brogden, Antimicrobial peptides: pore formers or metabolic inhibitors in bacteria, Nat. Rev. Microbiol. 3 (2005) 239–250.
[30] D.A. Devine, R.E.W. Hancock, Cationic peptides: distribution and mechanisms of resistance, Curr. Pharm. Des. 8 (2002) 703–714.
[31] S.H. Marshall, G. Arenas, Antimicrobial peptides: a natural alternative to chemical antibiotics and a potential for applied biotechnology, J. Biotechnol. 6 (2003) 272–284.
[32] Y. Shai, From innate immunity to de-novo designed antimicrobial peptides, Curr. Pharm. Des. 8 (2002) 715–725.
[33] W. van't Hof, E.C. Veerman, E.J. Helmerhorst, A. Nieuw, A.V., Antimicrobial peptides: properties and applicability, Biol. Chem., 382 (2001) 597–619.
[34] M. Zasloff, Antimicrobial peptides of multicellular organisms, Nature 415 (2002) 389–395.
[35] S.C. Mansour, O.M. Pena, R.E. Hancock, Host defense peptides: front-line immunomodulators, Trends Immunol. 35 (2014) 443–450.
[36] A.L. Hilchie, K. Wuerth, R.E. Hancock, Immune modulation by multifaceted cationic host defense (antimicrobial) peptides, Nat. Chem. Biol. 9 (2013) 761–768.
[37] E.F. Haney, R.E.W. Hancock, Peptide design for antimicrobial and immunomodulatory applications, Biopolymers 6 (2013) 572–583.
[38] C.D. Fjell, J.A. Hiss, R.E.W. Hancock, G. Schneider, Designing antimicrobial peptides: form follows function, Nat. Rev. Drug Disc. 11 (2012) 37–51.
[39] G. Diamond, N. Beckloff, A. Weinberg, K.O. Kisich, The roles of antimicrobial peptides in innate host defense, Curr. Pharm. Des. 15 (2009) 2377–2392.
[40] X. Lauth, H. Shike, J.C. Burns, M.E. Westerman, V.E. Ostland, J.M. Carlberg, J.C. Van Olst, V. Nizet, S.W. Taylor, C. Shimizu, P. Bulet, Discovery and characterization of two isoforms of moronecidin, a novel antimicrobial peptide from hybrid striped bass, J. Biol. Chem. 277 (2002) 5030–5039.
[41] E.J. Noga, U. Silphaduang, Piscidins: a novel family of peptide antibiotics from fish, Drug News Perspect. 16 (2003) 87–92.
[42] X. Lauth, J.J. Babon, J.A. Stannard, S. Singh, V. Nizet, J.M. Carlberg, V.E. Ostland, M.W. Pennington, R.S. Norton, M.E. Westerman, Bass hepcidin synthesis, solution structure, antimicrobial activities and synergism, and in vivo hepatic response to bacterial infections, J. Biol. Chem. 280 (2005) 9272–9282.
[43] B.S. Dezfuli, A. Lui, L. Giari, G. Castaldelli, V. Mulero, E.J. Noga, Infiltration and activation of acidophilic granulocytes in skin lesions of gilthead seabream, Sparus aurata, naturally infected with lymphocystis disease virus, Dev. Comp. Immunol. 36 (2012) 174–182.
[44] R.A. Festa, D.J. Thiele, Copper at the front line of the host-pathogen battle, PLoS Pathog. 8 (2012) e1002887.
[45] J.P. Mattila, K. Sabatini, P.K. Kinnunen, Oxidized phospholipids as potential molecular targets for antimicrobial peptides, Biochim. Biophys. Acta 1778 (2008) 2041–2050.
[46] A.K. Hauck, D.A. Bernlohr, Oxidative stress and lipotoxicity, J. Lipid Res. 57 (2016) 1976–1986.
[47] A. Ayala, M.F. Munoz, S. Arguelles, Lipid peroxidation: production, metabolism, and signaling mechanisms of malondialdehyde and 4-hydroxy-2-nonenal, Oxidative Med. Cell. Longev. 2014 (2014) 360438.
[48] K. Jomova, D. Vondrakova, M. Lawson, M. Valko, Metals, oxidative stress and neurodegenerative disorders, Mol. Cell. Biochem. 345 (2010) 91–104.
[49] S.F. AbdulSalam, F.S. Thowfeik, E.J. Merino, Excessive reactive oxygen species and exotic DNA lesions as an exploitable liability, Biochemistry 55 (2016) 5341–5352.
[50] P.K. Kinnunen, K. Kaarniranta, A.K. Mahalka, Protein-oxidized phospholipid interactions in cellular signaling for cell death: from biophysics to clinical correlations, Biochim. Biophys. Acta 1818 (2012) 2446–2455.
[51] R. Volinsky, P.K. Kinnunen, Oxidized phosphatidylcholines in membrane-level cellular signaling: from biophysics to physiology and molecular pathology, FEBS J. 280 (2013) 2806–2816.
[52] P. Jurkiewicz, A. Olzynska, L. Cwiklik, E. Conte, P. Jungwirth, F.M. Megli, M. Hof, Biophysics of lipid bilayers containing oxidatively modified phospholipids: insights from fluorescence and EPR experiments and from MD simulations, Biochim. Biophys. Acta 1818 (2012) 2388–2402.
[53] A.R. Moravec, A.W. Siv, C.R. Hobby, E.N. Lindsay, L.V. Norbash, D.J. Shults, S.J.K. Symes, D.K. Giles, Exogenous Polyunsaturated Fatty Acids Impact Membrane Remodeling and Affect Virulence Phenotypes among Pathogenic Vibrio Species, Appl. Environ. Microbiol. 83 (2017) e01415–17.
[54] L.Y. Baker, C.R. Hobby, A.W. Siv, W.C. Bible, M.S. Glennon, D.M. Anderson, S.J. Symes, D.K. Giles, Pseudomonas aeruginosa responds to exogenous polyunsaturated fatty acids (PUFAs) by modifying phospholipid composition, membrane permeability, and phenotypes associated with virulence, BMC Microbiol. 18 (2018) 117.
[55] L.H. Wang, X.A. Zeng, M.S. Wang, C.S. Brennan, D. Gong, Modification of membrane properties and fatty acids biosynthesis-related genes in Escherichia coli and Staphylococcus aureus: implications for the antibacterial mechanism of naringenin, Biochim. Biophys. Acta Biomembr. 1860 (2018) 481–490.
[56] A.K. Ulrich, D. de Mendoza, J.L. Garwin, J.E. Cronan Jr., Genetic and biochemical analyses of Escherichia coli mutants altered in the temperature-dependent regulation of membrane lipid composition, J. Bacteriol. 154 (1983) 221–230.
[57] K. Sabatini, J.P. Mattila, F.M. Megli, P.K. Kinnunen, Characterization of two oxidatively modified phospholipids in mixed monolayers with DPPC, Biophys. J. 90 (2006) 4488–4499.
[58] M. Wallgren, L. Beranova, Q.D. Pham, K. Linh, M. Lidman, J. Procek, K. Cyprych, P.K. Kinnunen, M. Hof, G. Grobner, Impact of oxidized phospholipids on the structural and dynamic organization of phospholipid membranes: a combined DSC and solid state NMR study, Faraday Discuss. 161 (2013) 499–513 (discussion 563-489).
[59] H. Khandelia, O.G. Mouritsen, Lipid gymnastics: evidence of complete acyl chain reversal in oxidized phospholipids from molecular simulations, Biophys. J. 96 (2009) 2734–2743.
[60] J.J. Knobloch, A.R. Nelson, I. Koper, M. James, D.J. McGillivray, Oxidative damage to biomimetic membrane systems: in situ Fe(II)/ascorbate initiated oxidation and incorporation of synthetic oxidized phospholipids, Langmuir 31 (2015) 12679–12687.
[61] H.L. Smith, M.C. Howland, A.W. Szmodis, Q. Li, L.L. Daemen, A.N. Parikh, J. Majewski, Early stages of oxidative stress-induced membrane permeabilization: a neutron reflectometry study, J. Am. Chem. Soc. 131 (2009) 3631–3638.
[62] H. Zhao, P. Kinnunen, Binding of the antimicrobial peptide temporin L to liposomes assessed by Trp fluorescence, J. Biol. Chem. 277 (2002) 25170–25177.
[63] J.C. Joyner, J.A. Cowan, Target-directed catalytic metallodrugs, Braz. J. Med. Biol. Res. 46 (2013) 465–485.
[64] S. Melino, C. Santone, P. Di Nardo, B. Sarkar, Histatins: salivary peptides with copper(II)- and zinc(II)-binding motifs: perspectives for biomedical applications, FEBS J. 281 (2014) 657–672.
[65] M.D.J. Libardo, V.Y. Gorbatyuk, A.M. Angeles-Boza, Central role of the copper-binding motif in the complex mechanism of action of Ixosin: enhancing oxidative damage and promoting synergy with Ixosin B, ACS Infectious Diseases 2 (2016) 71–81.
[66] M.D. Libardo, J.L. Cervantes, J.C. Salazar, A.M. Angeles-Boza, Improved bioactivity of antimicrobial peptides by addition of amino-terminal copper and nickel (ATCUN) binding motifs, ChemMedChem 9 (2014) 1892–1901.
[67] M.D. Libardo, T.J. Paul, R. Prabhakar, A.M. Angeles-Boza, Hybrid peptide ATCUN-sh-Buforin: influence of the ATCUN charge and stereochemistry on antimicrobial activity, Biochimie 113 (2015) 143–155.
[68] M.D. Libardo, S. Nagella, A. Lugo, S. Pierce, A.M. Angeles-Boza, Copper-binding tripeptide motif increases potency of the antimicrobial peptide Anoplin via reactive oxygen species generation, Biochem. Biophys. Res. Commun. 456 (2015) 446–451.
[69] U. Silphaduang, E.J. Noga, Peptide antibiotics in mast cells of fish, Nature 414 (2001) 268–269.
[70] J. Ruangsri, J.M.O. Fernandes, J. Rombout, M.F. Brinchmann, V. Kiron, Ubiquitous presence of piscidin-1 in Atlantic cod as evidenced by immunolocalisation, BMC Vet. Res. 8 (2012) 46.
[71] K.C. Peng, S.H. Lee, A.L. Hour, C.Y. Pan, L.H. Lee, J.Y. Chen, Five different piscidins from Nile Tilapia, Oreochromis niloticus: analysis of their expressions and biological functions, PLoS One 7 (2012) e50263.
[72] U. Silphaduang, A. Colorni, E.J. Noga, Evidence for widespread distribution of piscidin antimicrobial peptides in teleost fish, Dis. Aquat. Org. 72 (2006) 241–252.
[73] B.S. Perrin Jr., Y. Tian, R. Fu, C.V. Grant, E.Y. Chekmenev, W.E. Wieczorek, A.E. Dao, R.M. Hayden, C.M. Burzynski, R.M. Venable, M. Sharma, S.J. Opella, R.W. Pastor, M.L. Cotten, High-resolution structures and orientations of antimicrobial peptides piscidin 1 and piscidin 3 in fluid bilayers reveal tilting, kinking, and bilayer immersion, J. Am. Chem. Soc. 136 (2014) 3491–3504.
[74] A.A. De Angelis, C.V. Grant, M.K. Baxter, J.A. McGavin, S.J. Opella, M.L. Cotten, Amphipathic antimicrobial piscidin in magnetically aligned lipid bilayers, Biophys. J. 101 (2011) 1086–1094.
[75] R. Fu, E.D. Gordon, D.J. Hibbard, M. Cotten, High resolution heteronuclear correlation NMR spectroscopy of an antimicrobial peptide in aligned bilayers at high magnetic field: peptide-water interactions at the water-bilayer interface, J. Am. Chem. Soc. 131 (2009) 10830–10831.
[76] E.Y. Chekmenev, B.S. Vollmar, K.T. Forseth, M.N. Manion, S.M. Jones, T.J. Wagner, R.M. Endicott, B.P. Kyriss, L.M. Homem, M. Pate, J. He, J. Raines, P.L. Gor'kov, W.W. Brey, D.J. Mitchell, A.J. Auman, M. Ellard-Ivey, J. Blazyk, M. Cotten, Investigating molecular recognition and biological function at interfaces using piscidins, antimicrobial peptides from fish, Biochim. Biophys. Acta 1758 (2006) 1359–1372.
[77] S.A. Lee, Y.K. Kim, S.S. Lim, W.L. Zhu, H. Ko, S.Y. Shin, K.S. Hahm, Y. Kim,

Solution structure and cell selectivity of piscidin 1 and its analogues, Biochemistry 46 (2007) 3653–3663.
[78] S. Campagna, N. Saint, G. Molle, A. Aumelas, Structure and mechanism of action of the antimicrobial peptide piscidin, Biochemistry 46 (2007) 1771–1778.
[79] E. Lee, A. Shin, K.W. Jeong, B. Jin, H.N. Jnawali, S. Shin, S.Y. Shin, Y. Kim, Role of phenylalanine and valine10 residues in the antimicrobial activity and cytotoxicity of piscidin-1, PLoS One 9 (2014) e114453.
[80] H.-J. Lin, T.-C. Huang, S. Muthusamy, J.-F. Lee, Y.-F. Duann, C.-H. Lin, Piscidin-1, an Antimicrobial Peptide from Fish (Hybrid Striped Bass *Morone saxatilis* x *M. chrysops*), Induces Apoptotic and Necrotic Activity in HT1080 Cells, Zoolog. Sci., 29 (2012) 327–332.
[81] G. Wang, Database-guided discovery of potent peptides to combat HIV-1 or superbugs, Pharmaceuticals 6 (2013) 728–758.
[82] W.F. Chen, S.Y. Huang, C.Y. Liao, C.S. Sung, J.Y. Chen, Z.H. Wen, The use of the antimicrobial peptide piscidin (PCD)-1 as a novel anti-nociceptive agent, Biomaterials 53 (2015) 1–11.
[83] M. Mihailescu, M. Sorci, J. Seckute, V.I. Silin, J. Hammer, B.S. Perrin Jr., J.I. Hernandez, N. Smajic, A. Shrestha, K.A. Bogardus, A.I. Greenwood, R. Fu, J. Blazyk, R.W. Pastor, L.K. Nicholson, G. Belfort, M.L. Cotten, Structure and function in antimicrobial piscidins: histidine position, directionality of membrane insertion, and pH-dependent permeabilization, J. Am. Chem. Soc. 141 (2019) 9837–9853.
[84] S.Y. Kim, F. Zhang, W. Gong, K. Chen, K. Xia, F. Liu, R. Gross, J.M. Wang, R.J. Linhardt, M.L. Cotten, Copper regulates the interactions of antimicrobial piscidin peptides from fish mast cells with formyl peptide receptors and heparin, J. Biol. Chem. 293 (2018) 15381–15396.
[85] F. Comert, A. Greenwood, J. Maramba, R. Acevedo, L. Lucas, T. Kulasinghe, L.S. Cairns, Y. Wen, R. Fu, J. Hammer, J. Blazyk, S. Sukharev, M.L. Cotten, M. Mihailescu, The host-defense peptide piscidin P1 reorganizes lipid domains in membranes and decreases activation energies in mechanosensitive ion channels, J. Biol. Chem. 294 (2019) 18557–18570.
[86] M.D.J. Libardo, A.A. Bahar, B. Ma, R. Fu, L.E. McCormick, J. Zhao, S.A. McCallum, R. Nussinov, D. Ren, A.M. Angeles-Boza, M.L. Cotten, Nuclease activity gives an edge to host-defense peptide piscidin 3 over piscidin 1, rendering it more effective against persisters and biofilms, The FEBS J. 284 (2017) 3662–3683.
[87] R.K. Rai, A. De Angelis, A. Greenwood, S.J. Opella, M.L. Cotten, Metal-ion binding to host defense peptide Piscidin 3 observed in phospholipid bilayers by magic angle spinning solid-state NMR, Chemphyschem 20 (2018) 295–301.
[88] M. Wallgren, M. Lidman, Q.D. Pham, K. Cyprych, G. Grobner, The oxidized phospholipid PazePC modulates interactions between Bax and mitochondrial membranes, Biochim. Biophys. Acta 1818 (2012) 2718–2724.
[89] A. Oludiran, D.S. Courson, M.D. Stuart, A.R. Radwan, J.C. Poutsma, M.L. Cotten, E.B. Purcell, How oxygen availability affects the antimicrobial efficacy of host defense peptides: lessons learned from studying the copper-binding peptides piscidins 1 and 3, Int J Mol Sci 20 (2019) E5289.
[90] J.C. Stewart, Colorimetric determination of phospholipids with ammonium ferrothiocyanate, Anal. Biochem. 104 (1980) 10–14.
[91] T. Wieprecht, M. Beyermann, J. Seelig, Thermodynamics of the coil-alpha-helix transition of amphipathic peptides in a membrane environment: the role of vesicle curvature, Biophys. Chem. 96 (2002) 191–201.
[92] R. Friedman, Membrane-ion interactions, J. Membr. Biol. 251 (2018) 453–460.
[93] G. Gasmi, A. Singer, J. Forman-Kay, B. Sarkar, NMR structure of neuromedin C, a neurotransmitter with an amino terminal CuII-, NiII-binding (ATCUN) motif, J. Pept. Res. 49 (1997) 500–509.
[94] S. Melino, C. Santone, P. Di Nardo, B. Sarkar, Histatins: salivary peptides with copper(II)- and zinc(II)-binding motifs: perspectives for biomedical applications, FEBS J. 281 (2014) 657–672.
[95] S. Melino, M. Gallo, E. Trotta, F. Mondello, M. Paci, R. Petruzzelli, Metal-binding and nuclease activity of an antimicrobial peptide analogue of the salivary Histatin 5, Biochemistry 45 (2006) 15373–15383.
[96] H. Gusman, U. Lendenmann, J. Grogan, R.F. Troxler, F.G. Oppenheim, Is salivary histatin 5 a metallopeptide? Biochim. Biophys. Acta 1545 (2001) 86–95.
[97] P.L. Gor'kov, E.Y. Chekmenev, C. Li, M. Cotten, J.J. Buffy, N.J. Traaseth, G. Veglia, W.W. Brey, Using Low-E resonators to reduce RF heating in biological samples for static solid-state NMR up to 900 MHz, J. Magn. Reson. 185 (2007) 77–93.
[98] P.L. Gor'kov, E.Y. Chekmenev, R. Fu, J. Hu, T.A. Cross, M. Cotten, W.W. Brey, A large volume flat coil probe for oriented membrane proteins, J. Magn. Reson. 181 (2006) 9–20.
[99] H.W. Huang, Action of antimicrobial peptides: two-state model, Biochemistry 39 (2000) 8347–8352.
[100] R.M. Hayden, G.K. Goldberg, B.M. Ferguson, M.W. Schoeneck, M.D. Libardo, S.E. Mayeux, A. Shrestha, K.A. Bogardus, J. Hammer, S. Pryshchep, H.K. Lehman, M.L. McCormick, J. Blazyk, A.M. Angeles-Boza, R. Fu, M.L. Cotten, Complementary effects of host defense peptides Piscidin 1 and Piscidin 3 on DNA and lipid membranes: biophysical insights into contrasting biological activities, J. Phys. Chem. B 119 (2015) 15235–15246.
[101] S.A. Lee, Y.K. Kim, S.S. Lim, W.L. Zhu, H. Ko, S.Y. Shin, K. Hahm, Y. Kim, Solution structure and cell selectivity of piscidin 1 and its analogues, Biochemistry 46 (2007) 3653–3663.
[102] W.S. Sung, J.H. Lee, D.G. Lee, Fungicidal effect of piscidin on Candida albicans: pore formation in lipid vesicles and activity in fungal membranes, Biol. Pharm. Bull. 31 (2008) 1906–1910.
[103] Z. Jiang, A.I. Vasil, M.L. Vasil, R.S. Hodges, "specificity determinants" improve therapeutic indices of two antimicrobial peptides Piscidin 1 and Dermaseptin S4 against the gram-negative pathogens Acinetobacter baumannii and Pseudomonas aeruginosa, Pharmaceuticals (Basel) 7 (2014) 366–391.
[104] M. Ouellet, G. Bernard, N. Voyer, M. Auger, Insights on the interactions of synthetic amphipathic peptides with model membranes as revealed by 31P and 2H solid-state NMR and infrared spectroscopies, Biophys. J. 90 (2006) 4071–4084.
[105] M.S. Balla, J.H. Bowie, F. Separovic, Solid-state NMR study of antimicrobial peptides from Australian frogs in phospholipid membranes, Eur. Biophys. J. 33 (2004) 109–116.
[106] B. Antonny, Mechanisms of membrane curvature sensing, Annu. Rev. Biochem. 80 (2011) 101–123.
[107] G. Drin, J.F. Casella, R. Gautier, T. Boehmer, T.U. Schwartz, B. Antonny, A general amphipathic alpha-helical motif for sensing membrane curvature, Nat. Struct. Mol. Biol. 14 (2007) 138–146.
[108] J. Zimmerberg, M.M. Kozlov, How proteins produce cellular membrane curvature, Nat. Rev. Mol. Cell Biol. 7 (2006) 9–19.
[109] K. Hristova, W.C. Wimley, V.K. Mishra, G.M. Anantharamiah, J.P. Segrest, S.H. White, An amphipathic alpha-helix at a membrane interface: a structural study using a novel X-ray diffraction method, J. Mol. Biol. 290 (1999) 99–117.
[110] J. Seelig, Thermodynamics of lipid–peptide interactions, Biochim. Biophys. Acta Biomembr. 1666 (2004) 40–50.
[111] E. Kuchinka, J. Seelig, Interaction of melittin with phosphatidylcholine membranes. Binding isotherm and lipid head-group conformation, Biochemistry 28 (1989) 4216–4221.
[112] J. Kozlowska, L.S. Vermeer, G.B. Rogers, N. Rehnnuma, S.B. Amos, G. Koller, M. McArthur, K.D. Bruce, A.J. Mason, Combined systems approaches reveal highly plastic responses to antimicrobial peptide challenge in Escherichia coli, PLoS Pathog. 10 (2014) e1004104.
[113] D. Roversi, V. Luca, S. Aureli, Y. Park, M.L. Mangoni, L. Stella, How many antimicrobial peptide molecules kill a bacterium? The case of PMAP-23, ACS Chem. Biol. 9 (2014) 2003–2007.
[114] H. Choi, Z. Yang, J.C. Weisshaar, Single-cell, real-time detection of oxidative stress induced in Escherichia coli by the antimicrobial peptide CM15, Proc. Natl. Acad. Sci. U. S. A. 112 (2015) E303–E310.
[115] T.C. Vogt, B. Bechinger, The interactions of histidine-containing amphipathic helical peptide antibiotics with lipid bilayers. The effects of charges and pH, J. Biol. Chem., 274 (1999) 29115–29221.
[116] C.S. Pearson, Z. Kloos, B. Murray, E. Tabe, M. Gupta, J.H. Kwak, P. Karande, K.A. McDonough, G. Belfort, Combined bioinformatic and rational design approach to develop antimicrobial peptides against Mycobacterium tuberculosis, Antimicrob. Agents Chemother. 60 (2016) 2757–2764.
[117] J. Seelig, P.M. Macdonald, P.G. Scherer, Phospholipid head groups as sensors of electric charge in membranes, Biochemistry 26 (1987) 7535–7541.
[118] Y. Su, W.F. DeGrado, M. Hong, Orientation, dynamics, and lipid interaction of an antimicrobial arylamide investigated by 19F and 31P solid-state NMR spectroscopy, J. Am. Chem. Soc. 132 (2010) 9197–9205.
[119] K.A. Henzler-Wildman, D.K. Lee, A. Ramamoorthy, Mechanism of lipid bilayer disruption by the human antimicrobial peptide, LL-37, Biochemistry 42 (2003) 6545–6558.
[120] B. Bechinger, E.S. Salnikov, The membrane interactions of antimicrobial peptides revealed by solid-state NMR spectroscopy, Chem. Phys. Lipids 165 (2012) 282–301.
[121] M. Ouellet, F. Otis, N. Voyer, M. Auger, Biophysical studies of the interactions between 14-mer and 21-mer model amphipathic peptides and membranes: insights on their modes of action, Biochim. Biophys. Acta Biomembr. 1758 (2006) 1235–1244.
[122] P. Tremouilhac, E. Strandberg, P. Wadhwani, A.S. Ulrich, Conditions affecting the re-alignment of the antimicrobial peptide PGLa in membranes as monitored by solid state 2H-NMR, Biochim. Biophys. Acta 1758 (2006) 1330–1342.
[123] W.K.I Marcotte, YH Lam, BC Chia, MR de Planque, JH Bowie, M Auger, F. Separovic, Interaction of antimicrobial peptides from Australian amphibians with lipid membranes, Chem Phys Lipids 122 (2003) 107–120.
[124] C. Harford, B. Sarkar, Amino terminal Cu(II)- and Ni(II)-binding (ATCUN) motif of proteins and peptides: metal binding, DNA cleavage, and other properties, Acc. Chem. Res. 30 (1997) 123–130.
[125] J. Seelig, ^{31}P nuclear magnetic resonance and the head group structure of phospholipids in membranes, Biochim. Biophys. Acta 515 (1978) 105–140.
[126] D.M. Grant, Chemical shift tensors, in: D.M. Grant (Ed.), Encyclopedia of Nuclear Magnetic Resonance, J. Wiley, Chichester/New York, 1996, pp. 1298–1321.
[127] M. Auger, Membrane structure and dynamics as viewed by solid-state NMR spectroscopy, Biophys. Chem. 68 (1997) 233–241.
[128] B. Bechinger, Detergent-like properties of magainin antibiotic peptides: a 31P solid-state NMR spectroscopy study, Biochim. Biophys. Acta 1712 (2005) 101–108.
[129] I. Moll, F., T.A. Cross, Optimizing and characterizing alignment of oriented lipid bilayers containing gramicidin D, Biophys. J., 57 (1990) 351–362.
[130] A. Ramamoorthy, S. Thennarasu, D.K. Lee, A. Tan, L. Maloy, Solid-state NMR investigation of the membrane-disrupting mechanism of antimicrobial peptides MSI-78 and MSI-594 derived from magainin 2 and melittin, Biophys. J. 91 (2006) 206–216.
[131] S.J. Opella, NMR and membrane proteins, Nat. Struct. Biol. 4 (1997) 845–848.
[132] F.M. Marassi, S.J. Opella, NMR structural studies of membrane proteins, Curr. Opin. Struct. Biol. 8 (1998) 640–648.
[133] B. Bechinger, Biophysical investigations of membrane perturbations by polypeptides using solid-state NMR spectroscopy, Mol. Membr. Biol. 17 (2000) 135–142.

[134] S.A. Juliano, S. Pierce, J.A. deMayo, M.J. Balunas, A.M. Angeles-Boza, Exploration of the Innate Immune System of *Styela clava*: Zn(2+) Binding Enhances the Antimicrobial Activity of the Tunicate Peptide Clavanin A, Biochemistry, 56 (2017) 1403–1414.
[135] B.S. Perrin, R. Fu, M.L. Cotten, R.W. Pastor, Simulations of membrane-disrupting peptides II: AMP piscidin 1 favors surface defects over pores, Biophys. J. 111 (2016) 1258–1266.
[136] L. Guo, K.B. Smith-Dupont, F. Gai, Diffusion as a probe of peptide-induced membrane domain formation, Biochemistry 50 (2011) 2291–2297.
[137] F. Hane, G. Tran, S.J. Attwood, Z. Leonenko, Cu(2+) affects amyloid-beta (1-42) aggregation by increasing peptide-peptide binding forces, PLoS One 8 (2013) e59005.
[138] I. Mulero, E.J. Noga, J. Meseguer, A. Garcia-Ayala, V. Mulero, The antimicrobial peptides piscidins are stored in the granules of professional phagocytic granulocytes of fish and are delivered to the bacteria-containing phagosome upon phagocytosis, Dev. Comp. Immunol. 32 (2008) 1531–1538.